BeFo
STIFTELSEN BERGTEKNISK FORSKNING
ROCK ENGINEERING RESEARCH FOUNDATION

DEVELOPMENT OF DYNAMIC GROUTING STAGE 2

Ojas Arun Chaudhari
Giedrius Zirgulis

BeFo Report 237

STIFTELSEN BERGTEKNISK FORSKNING
ROCK ENGINEERING RESEARCH FOUNDATION

DEVELOPMENT OF DYNAMIC GROUTING STAGE 2

Utveckling av dynamisk injektering Etapp 2

Ojas Arun Chaudhari, RISE

Giedrius Zirgulis, RISE

BeFo Report 237
Stockholm 2023
ISSN1104-1773
ISRN BEFO-R-237-SE

PREFACE

Water ingress into the subsurface infrastructures from the surrounding formations may lead to several environmental, economic and sustainability problems. Sufficient spread of grout in rock fractures is necessary for obtaining the required sealing of the rock fractures. Previous projects at the lab-scale level showed that dynamic grouting improved the spread of the grout in the microfractures substantially. This project has investigated development of the dynamic grouting under field conditions at the SKB facility Äspö HRL, i.e., in an actual tunnel. The efficiency of the new dynamic injection technique adapted from lab-scale experiments to field applications was verified.

The project work was carried out by the department of Infrastructure and Concreting at Research Institutes of Sweden (RISE). The primary working group consisted of Ojas Chaudhari (Material Design, RISE) as project leader and Giedrius Zirgulis (Material lab., RISE). In addition, the working group consisted of Almir Draganovic (SKB), Ulf Håkansson (Skanska), Tommy Ellison (Besab) and Anders Selander (Cementa). The main work (laboratory Stage 1) and (field Stage 2) was conducted in the close collaboration with the participants from SKB and Skanska. Their expertise and experiences in the areas of dynamic grouting, grout penetrability, rheological properties and the grouting operations in the field has been of vital importance for the success of the project. The participants from Besab and Cementa contributed substantially at technical meetings and to the field tests, based on their extensive experiences in relation to the field operations and the materials.

The projects reference group consisted of Per Tengborg and Patrik Vidstrand (BeFo), Thomas Dalmalm (TRV), Peter Ulriksen (LTH), Charlotte Svensson Tengberg (Skanska) and Johan Funehag (Tyrens). Their in-kind support is greatly appreciated.

Stockholm

Patrik Vidstrand

FÖRORD

Vattnets inträning i underjordiska strukturer från omgivande miljö kan leda till flera miljö-, ekonomi- och hållbarhets problem. Tillräcklig inträngning av injekteringsbruk i bergssprickor är nödvändigt för att uppnå erforderlig tätning av bergmaterial. I tidigare projekt, som varit på laboratorienivå, visades att dynamisk injektering förbättrade inträngingen av injekteringsbruk i mikrosprickor avsevärt. Detta forskningsprojekt har vidareutvecklade den dynamiska injekteringsmetoden i fält vid SKB:s anläggning Äspö HRL dvs i en verklig tunnel. Projektet har verifierade effektiviteten av denna nya injekteringsteknik genom att utföra injekteringsförsök i fält.

Arbetet i projektet har utfösts av avdelningen Infrastruktur och betongbyggande vid Research Institutes of Sweden (RISE). Den primära arbetsgruppen bestod av Ojas Chaudhari (Material Design, RISE) projektledare och Giedrius Zirgulis (Material., RISE). I arbetsgruppen för projektet ingick dessutom Almir Draganovic (SKB), Ulf Håkansson (Skanska), Tommy Ellison (Besab) och Anders Selander (Cementa). Huvudarbetet (laboratorieundersökningar, Steg 1 och fältprovning, Steg 2) utfördes i nära samarbete med projektdeltagarna från SKB och Skanska. Deras expertis och erfarenheter inom dynamisk injektering, injekteringsmedels inträngning, reologiska egenskaper och injekteringsuppdrag i fält har bidragit till projektets framgång. Även deltagarna från Besab och Cementa har, baserat på lång erfarenhet av fältprovningar och materialkunskap, positivt bidragit till projektet vid tekniska möten och i samband med fältprovningen

Per Tengborg och Patrik Vidstrand (BeFo), Thomas Dalmalm (TRV), Peter Ulriksen (LTH), Charlotte Svensson Tengberg (Skanska) och Johan Funehag (Tyrens) har som referensgrupp utgjort ett viktigt stöd för projektet. Deras in-kind insatser uppskattas mycket.

Stockholm,

Patrik Vidstrand

SUMMARY

The water ingress into subsurface infrastructures from the surrounding environment may lead to environmental, economic, and sustainability problems. Sufficient spread of grout in rock fractures is necessary for obtaining the required sealing of the rock fractures. In the BeFo reports 149, 181, and 197 (Ghafar et al., 2015; Ghafar et al., 2017; Ghafar et al., 2019) it was shown that at lab-scale, dynamic grouting substantially improved the spread of grout in the microfractures. The initial experimental set ups consisted of short-slot and long-slot along with a gas-tank as the pressure source.

The aim of this project is to develop the dynamic grouting further for use in the field. The project has verified the efficiency of the innovative dynamic grouting technique by adapting previous lab-scale experiences to the field scale applications. The proposed method consisted of the applied pressure variation during the grout injection, and it varied from the method included in Ulriksen (2020).

In this project, an innovative grout distributor unit was developed and tested in the lab. The distributor unit was used to provide the dynamic pressure in multiple boreholes in sequence to improve the spread of the grout in rock fractures and to reduce the grouting time. Furthermore, the technique was examined at the Äspö HRL using the distributor unit and the testing set up to study potential issues that may occur during grouting and to demonstrate the effectiveness of the method under field conditions.

Unique experience was gathered by combining a distributor unit, laboratory sensors with an industrial injection system while performing the static and dynamic grouting under field conditions. The field test led to understanding the importance of several parameters, such as application of the special flow and pressure controllers for measuring grout properties, application of control valves for controlling dynamic and static pressure during the grouting operation. In addition, the interference of pressure distribution between adjacent boreholes gave valuable insights for the injection technique. Finally, the innovative dynamic injection approach showed promising results in form of increasing injection pressure.

Keywords: dynamic injection, grouting, grouting technology, field test

SAMMANFATTNING

Vattnets inträning i underjordiska strukturer från omgivande miljö leder till flera miljö-, ekonomi- och hållbarhetsfrågor. Tillräcklig spridning av injekteringsbruk i bergssprickor är nödvändigt för att få erforderlig tätning av bergmaterial. I BeFos rapporter 149, 181 och 197 ((Ghafar et al., 2015; Ghafar et al., 2017; Ghafar et al., 2019) står det att i laboratorieskala förbättrar dynamiska injektering avsevärt spridningen av injekteringsbruk i mikrosprickor. Dessa initiala experiment bestod av kort-slot och lång-slot tillsammans med en tryckkälla, i detta fall en gastank.

Detta projekt syftar till att vidareutveckla den dynamiska injekteringen i fält. I projektet har effektiviteten hos effektiviteten hos den innovativa dynamiska injekteringstekniken varierats genom att anpassa tidigare erfarenheter i laboratorieskala till applikation i fältskala. Den föreslagna metoden bestod av den applicerade tryckvariationen under injekteringsbruket och den varierade från metoden som ingick Ulriksen (2020).

I detta projekt utvecklades och testades en innovativ fördelarenhet för injekteringsbruk i laboratoriet. Fördelarenheten användes för att fördela det dynamiska trycket över flera borrhålen i sekvens för att förbättra inträngningen av injekteringsbruket i berget och för att minska injekteringstiden. Vidare har tekniken undersökts vid Äspölaboratoriet med hjälp av fördelarenheten och testuppsättningen för att studera potentiella problem vid injektering och för att visa metodens effektivitet i fälttillämpningar.

Unika erfarenheter har samlats genom att kombinera en fördelningsenhet, laboratoriesensorer med ett industriellt injektionssystem samtidigt som den statiska och dynamiska injekteringen utförs i fält. Fälttestet gav förståelse när det gäller flera parametrar, såsom tillämpning av de speciella flödes- och tryckregulatorerna för mätning av injekteringsbruksegenskaper, tillämpning av styrning av ventiler för styrning av dynamiskt och statiskt tryck under injekteringstillfället. Dessutom gav interferensen av tryckfördelningen mellan intilliggande borrhål värdefulla insikter för injektionstekniken. Slutligen visade den innovativa dynamiska injekteringsmetoden lovande resultat i form av det ökande injektionstrycket.

Nyckelord: dynamisk injektering, injekteringsbruk, injekteringsteknik, fältprovning

CONTENTS

1. INTRODUCTION

To obtain sealing of underground structures against water penetrating from the surrounding environment, sufficient spread of the grout in rock fractures is an important parameter. For this purpose, cement-based grouts are used by the grouting industry worldwide. However, cement-based grout may lead to filtration of cement particles that restrict the grout from spreading in the rock fracture system (Draganović and Stille, 2011). Several years of laboratory investigations and field experiences have showed that the filtration tendency of the grout is governed by the applied pressure during grouting operation. During grouting operations, a certain increase in the applied pressure decreases the filtration and improves the spreading of the grout in the rock fractures. It was found that an incremental pressure increase was beneficial for the spread of the grout (Nobuto et al., 2008, Pusch et al., 1985). Further improvement of this technique can be obtained using high-frequency and large-amplitude oscillating pressure. This pressure superimposed on an underlying pressure allowed penetration of a low water content cement grout through 100 µm artificial fractures (Mohammed et al., 2015). Even though these studies are promising, the dynamic grouting using high-frequency oscillating pressure has not yet been industrialized due to the limited efficiency and quick dissipation of the high-frequency oscillations along a fracture.

As an alternative to the previous efforts using high-frequency oscillating pressure, a low-frequency rectangular pressure impulse was introduced in a recent study to increase the efficiency of the method, and to reduce the dissipation of the pressure impulses along a fracture (Ghafar et al., 2016). The results showed a significant improvement of the grouting spread. Up to 11 times more of the total volume of grout passed through the 30-43 µm slots (Ghafar et al., 2016). In addition, the dissipation of the pressure impulses was also studied in a considerably longer artificial fracture with 4 m length and apertures of 230 to 10 µm (Ghafar et al., 2017). In this case, dynamic pressure conditions improved the spread compared to static pressure conditions, and up to 11 times more of the total grout volume passed through apertures ≤ 70 µm.

The aim of this work is to develop dynamic grouting in the field-scale, maximize the efficiency of the new technique and adapt recent knowledge obtained in lab-scale tests to field application so that this new technique can be used in tunnel construction.

1.1 Main objectives

The project has two main objectives:

1. Verification of the efficiency of the method under controlled conditions in the laboratory
2. Demonstration of the effectiveness of the method in the field

Based on the objectives, the project was divided into two stages:

- Stage 1: Design, production, and pilot testing of the distribution unit
- Stage 2: Field-scale experiments at the Äspö Hard Rock Laboratory (Äspö HRL).

The aim was to increase the spread of injection grout in micro fractures ≤ 70 µm and to reduce the time necessary for grouting by combining two injection techniques: dynamic grouting and multiple borehole grouting. In stage 1, a distributor unit was to be developed, which could change the static pressure of a regular grouting pump to a dynamic pressure and could supply grout to multiple boreholes in sequence in order to increase the grout spread and to simultaneously to reduce the grouting time. This device was to be tested in the lab to assure its performance and to examine the overall aspects of the system. In stage 2, the efficiency of the method was to be investigated in full-scale at Äspö HRL using different pressure setups with various borehole arrangements. Hydrology tests were performed to study fracture tendency and connectivity of the boreholes. Selected boreholes were to be injected using the dynamic and a static method and flow rate and pressure of the injected grout should be measured.

The detail of each stage is described in the following section.

2. STAGE 1: DESIGN, PRODUCTION, AND PILOT TEST OF THE DISTRIBUTION UNIT IN THE LAB

2.1 The distribution unit

The aim was to build a pressure-distribution unit to transform the static pressure resulting from a regular grouting pump to a programmable dynamic pressure. Also, it required to distribute the applied pressure between multiple boreholes in sequence. It was intended to combine two techniques, the dynamic grouting, and the multiple-borehole grouting, to increase the grout spread and reduce the grouting time simultaneously. The pilot tests were carried out in the lab to assured that the system worked properly before testing in the field. A preliminary design of the distribution unit is presented in Figure 1 and it shows that there is a single inlet at the top connected to the grouting pump and four outlets at the bottom directing grouts towards the borehole. The number of active outlets necessary depends on the multiple factors, such as tunnel diameter, geological conditions of the ground, and spacing between the boreholes.

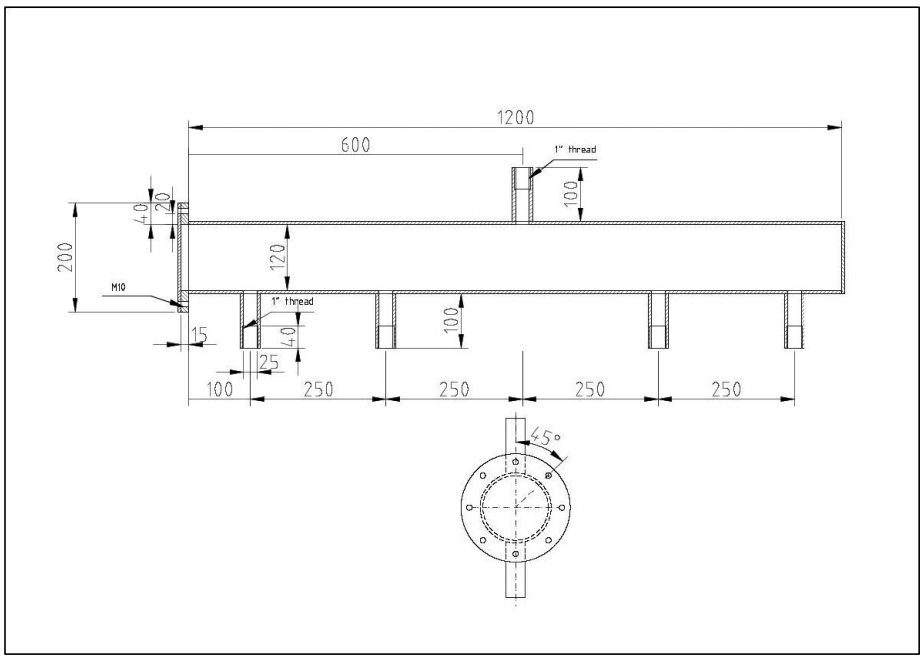

Figure 1. Design of distribution unit for grout injection.

During the dynamic grouting operation, the pressure increase for each outlet was achieved by opening the pressure valve allowing the grout to flow through the outlet. Then, the respective borehole was connected to a bypass valve which caused the pressure to drop instantaneously (approximately to zero) which caused a slight grout backflow. In this

dynamic method, the partially plugged constrictions were anticipated to be reopened for further penetration due to erosion of the filter cakes. The details of the laboratory are described in the following sections.

2.2 Raw materials and grout preparation

For the grout mix cement, water, and a superplasticizer was used. The cement type was a low alkali CEM I 525N–SR 3 LA with a particle size distribution of ≤ 30 µm (for 95% of the material), which is a cement normally used for injection grout in Sweden. The water to cement ratio was 0.8 and the superplasticizer dosage was 0.5 % by mass of cement. The grout was mixed with a high shear VMA mixer with dispersion disk. This mixer ensured appropriate dispersion of the grout components. The shear loads that it implied on the mix was similar to the shear loads of a colloidal mixing device that is used in the field. When the raw materials were added to the mix the speed was set to 2000 rpm for 1 minute and then it was increased to 10000 rpm for another 6 minutes. The mixing procedure was designed based on experiences from previous projects so that good dispersion of the material in grout should be achieved. The laboratory tests were performed using a maximum batch size of 12 liters. The quality of each mix was controlled using Marsh cone method (Figure **2**a) and filter pump test according to standard SS-EN 14497:2004/AC:2006 (European standard, 2006). As seen from Figure 2a, a Marsh cone time ≤ 35 sec was achieved. Similarly, Figure 2b filter pump testing shows that the grout passed through 63 µm aperture.

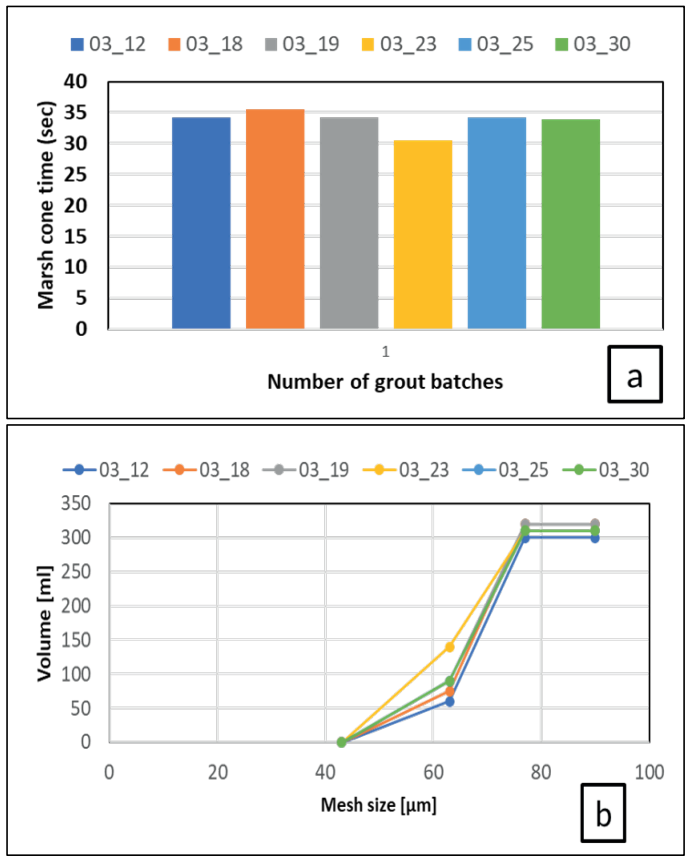

Figure 2. Test results from 6 grout injection experiments performed in the laboratory: a) Marsh cone time (b) Filter pump test

2.3 Test set up

To simulate the fractures formations in the rock a test rig, Variable Aperture Long Slot (VALS), was used (Ghafar et al., 2017), (Figure 3a). It consisted of two 4 m long steel plates with gradually diminishing apertures sizes from 230 µm to 10 µm (Figure 3b). The VALS also consisted of 500 µm chambers Before and after of each aperture there was a chamber with an aperture size of 500 µm, intended to simulate irregularities in the fracture width in real rocks.

The length of the apertures and the chambers was 180 mm, except for the one 10 µm aperture. This aperture had a length of 90 mm, and it was followed by 500 µm chamber with a length of 40 mm. The inlet to the VALS was placed before the 230 µm aperture (Figure 3b).

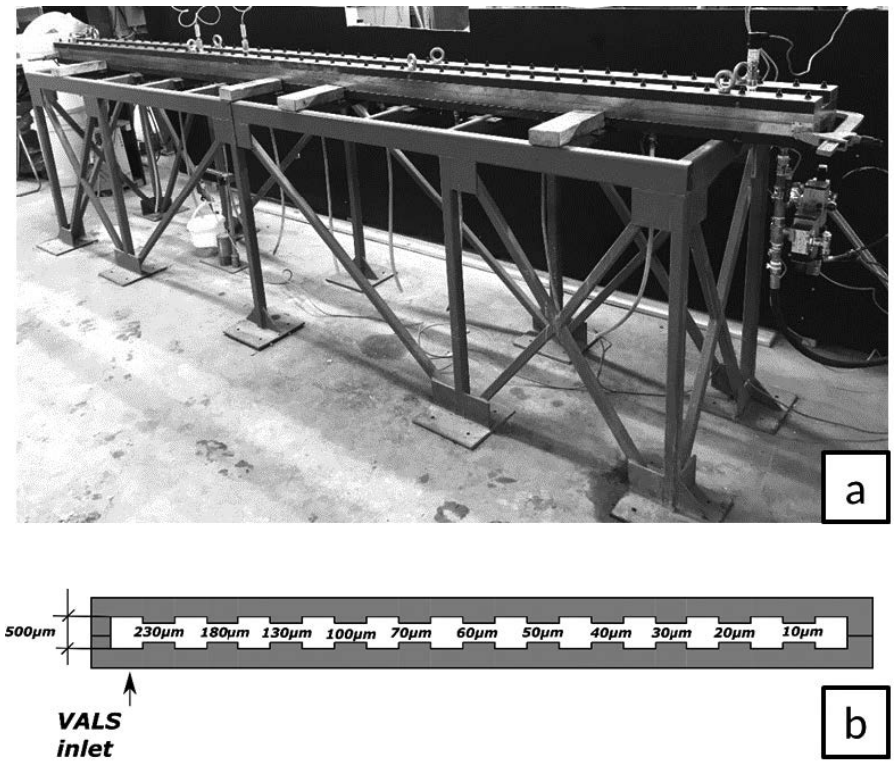

Figure 3. Device for laboratory test: a) Variable Aperture Long Slot (VALS) b) schematics of aperture sizes and distribution.

The grout distributor (Figure 4a) had four grout outflows, making it possible to inject four boreholes at a time during the field test. However, during the laboratory test, only one outflow was used. The grout distributor unit (Figure 4a) also served as a grout container (12 l) for laboratory tests. During the tests the grout distributor unit was filled with grout, which it delivered for the testing. It should be noted that the duration of the laboratory tests duration was defined by the capacity of the grout distributor.

During testing, pressure in the grout was created using compressed nitrogen gas connected to the grout distributor through the pressure regulator unit. The pressure profile of the grout (either dynamic or static) flowing towards the VALS inlet was regulated by grout control valves (Figure 4c). The grout control valves received signals from the valves control unit (Figure 4b), which consisted of open source an Arduino controller board. The board was connected to a relay block and controlled the opening and closing time for the pneumatic valves through a computer program. The Figure 5 shows a schematic picture of the complete set up for laboratory testing.

The Pressure and mass sensors were used to give out-put from the test (Figure 4c). During the test the change of the mass of the grout (flowing into the bucket) was measured using a mass sensor, which was located under the respective aperture valves in bottom part of the VALS (Figure 3). The aperture valves were opened and closed manually (by hand) during the test. The pressure sensor was used to record the pressure of the gas and the grout. The signals from pressure and mass sensors were recorded by a data acquisition system (DAQ) (Figure 5).

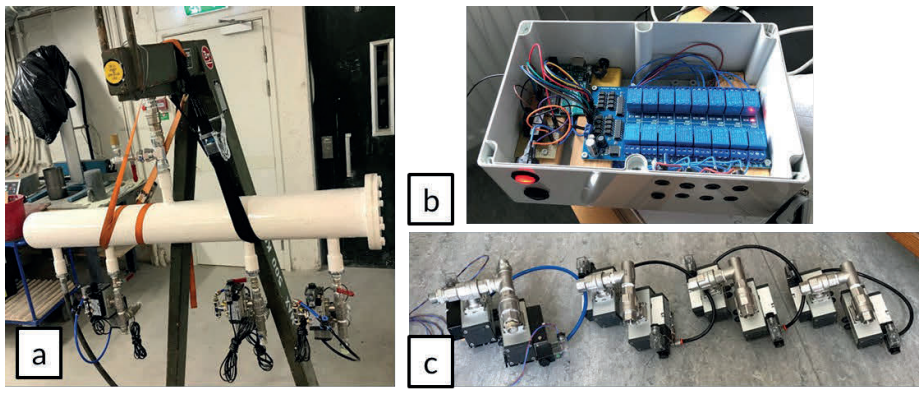

Figure 4. Parts of the testing set up: a) Grout distribution unit b) Pneumatic valves control unit consisting of an Arduino board and a relay block c) Pneumatic valves system.

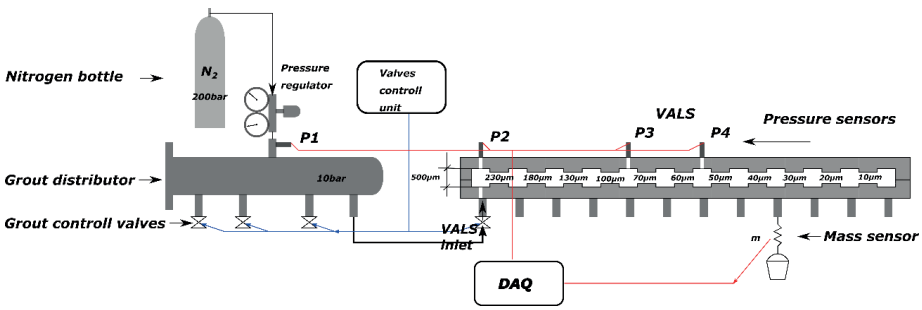

Figure 5 A schematic representation of the test set-up: A nitrogen gas tank connected to the grout distributor through a pressure regulating valve, VALS, mass and pressure sensors connected to DAQ system and grout pressure control valves connected to a control unit.

2.4 Experiments on VALS

During the tests, the opening time for the pneumatic valves (located under VALS) depended on the observed flow rate and was varied from 60 to 180 sec. The measurements in the tests were at a small aperture (40 µm) and continued towards the highest aperture (180 µm). Only one valve was allowed to stay open at a time. The long duration measurements (~180 sec) were used for small apertures in the range 40-70 µm, while the shortest duration measurements (~60 sec) were performed for large apertures in the range 100-180 µm. A total of six tests were performed: three with dynamic injection and three with static injection. It was observed that at the large size apertures, the grout displayed high flow rate for both the dynamic and the static injection regime, therefore it required shorter measurement time. Also, the pressure pulses for the dynamic injection regime lasted for two seconds after the opening of the grout control valve (Figure 4c) and then it was zero for 4 - 6 seconds (idle period). This cycle was repeated during the test duration (Figure 6).

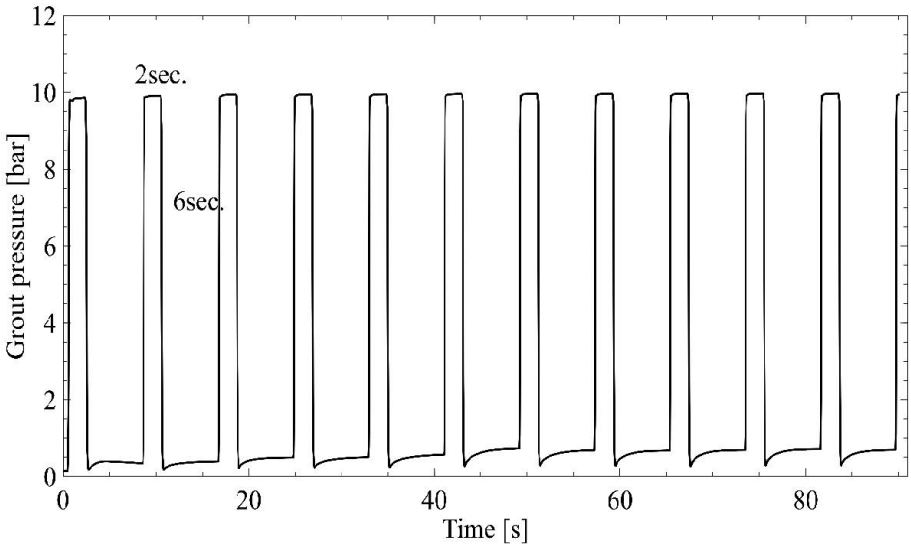

Figure 6 The grout pressure profile at the inlet to VALS during the dynamic pressure test**.**

2.5 Results

Figure 7 shows a typical grout flow profile under the dynamic injection regime. The profile consisted of inclined parts, displaying the injection rate and horizontal parts occurring during the idle period. For the data analysis, the idle period was removed, and the average flow rate was calculated. From the flow measurements, the average of the

flow rate of the grout was calculated for each aperture size (Figure 8). The results show that the grout flow rate was increased for the dynamic injection compared to the static injection regime. The key findings were observed for the apertures of 60 µm and 70 µm size, in which almost zero flow rate was observed for the static injection regime, which can be attributed to filter cake formation (Figure 8), whereas, significant flow (~4 g/l) was observed for the dynamic injection regime.

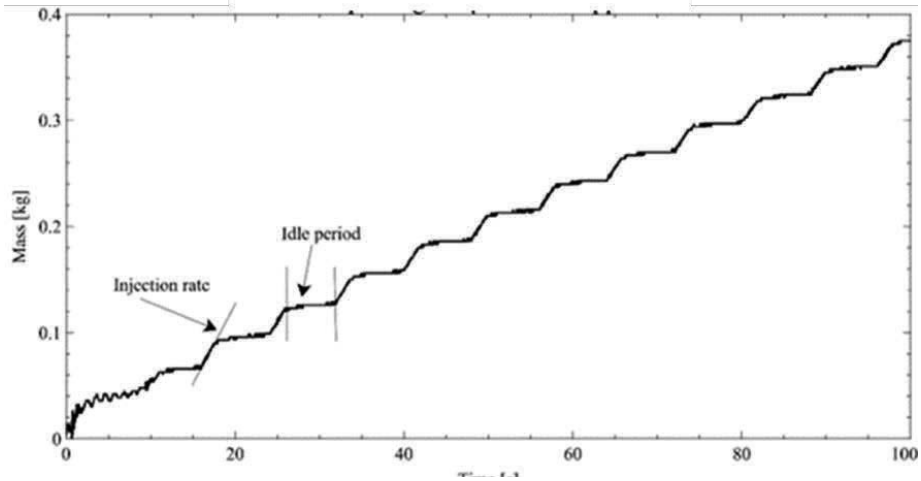

Figure 7 Typical profile for grout passing through 100 µm size aperture under the dynamic pressure regime**.**

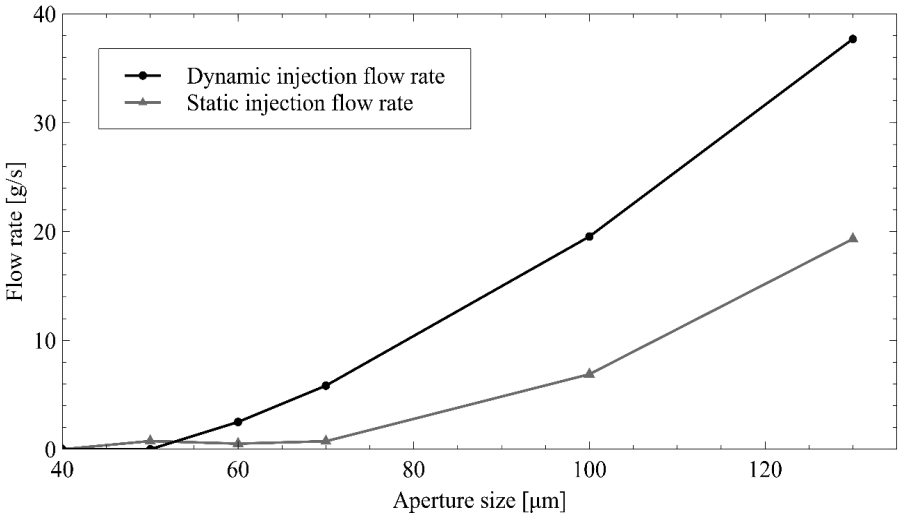

Figure 8. Average flow rate at various aperture sizes for dynamic injection and static injection.

3. STAGE 2 FIELD-SCALE EXPERIMENTS

3.1 General

The efficiency of the new technique was investigated in full-scale at Äspö HRL, where the locations for tests was selected based on the knowledge of the geological and hydrogeological conditions. The search of a suitable location for the field test carried out in cooperation with the project partners, and a few potential locations with good permeability and a fracture network in the rock were selected. Figure 9 shows a schematic representation of a grouting fan (shape as fan) with four grouting boreholes G1-G4 and four observational boreholes O1-O4. In the project proposal, the observational boreholes were mentioned but in the actual tests, the observational boreholes were not drilled due to space limitation. The brown circles in Figure 9, represented the two-dimensional spread of the grout around each grouting borehole. The graphs for the anticipated pressure variation in each borehole is also shown in Figure 9 (to the right). This pressure variation plot suggests that the grout pump could work without pressure change, if the provided pressure was distributed between the grouting boreholes. This schematic representation of a grouting fan with four boreholes was considered as an example. The schematic representation can be modified for more boreholes which can be grouted simultaneously. The effectiveness of the method to control filtration of grout was evaluated by measuring the flow and the pressure of the grout.

The details of the field testing for dynamic and static grouting are described in the following sections.

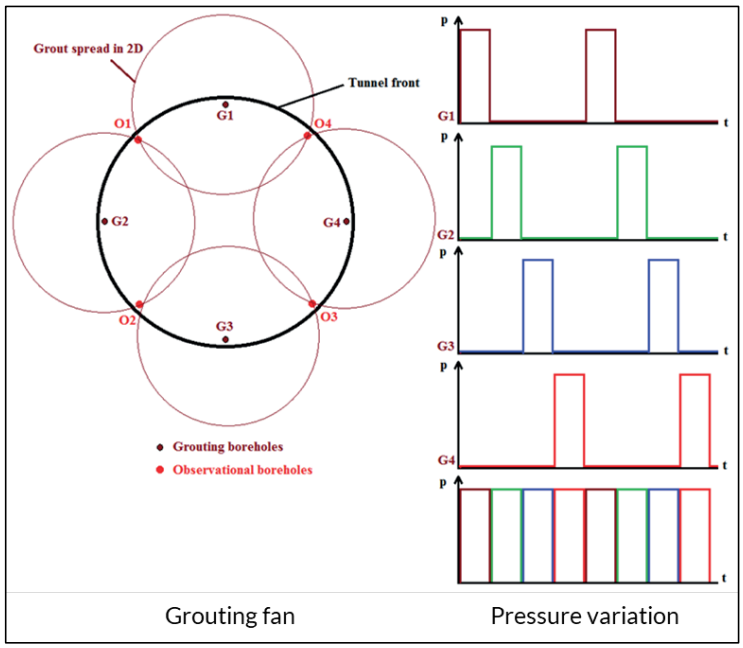

Figure 9 Schematic representation of a grouting fan with four grouting boreholes G1-G4 and four observational boreholes O1-O4 and the pressure variation in each grouting borehole.

3.2 Site selection for the field test

The previous projects with the field tests indicated that selection of a suitable site was the crucial and challenging task in the project. If the site is selected a site with ongoing constructions, the field experiment may be affected by the production routines at the site and can be disturbed by construction work (e.g., drilling operation of nearby rock). The test duration can also be highly dependent on the production schedule at the construction site. Thus, it was decided to contact SKB's Äspö Hard Rock Laboratory (Figeholm, Sweden) and after their positive reply, the field test planning could continue with the following steps: 1. site inspection 2. choosing final test site 3. drilling of boreholes 4. the testing.

3.2.1 Location search at Äspö HRL

The Äspö HRL consists of multiple tunnels which are situated at various depths. For initial screening for a suitable location, various aspects such as rock with interconnected fractures, accessible for drilling and grouting were considered. Eight possible sites at Äspö HRL were inspected (Table 1). The brief description of each site is given in the following sections.

Table 1 The list of the possible sites at Äspö HRL.

Number	Äspö HRL site name	Altitude of site from surface (m)
1	TAS05	400
2	TAS 04	400
3	Elevator	220
4	NASA0748	n/a
5	REDOX (TASR)	n/a
6	NASA0408A	n/a
7	TASM	n/a
8	NASA 0249A	~30

3.2.1.1 TAS05 (depth: ~400m)

The first probable candidate was site TAS05 (Figure 10a). This site contained few places with rocks with multiple fractures, which were clearly visible due to water seepage from the fractures. However, it was found that it would be difficult to drill and grout at this site because it was used for shotcrete applications.

Figure 10. Site inspection at ~400 m: a) site TAS05 b) site TAS04 general view c) site TAS04 water ingress on tunnel floor.

3.2.1.2 TAS04 (depth: ~400m)

The second site TAS04 (Figure 10b) was also located at ~400 m. Water ingress was visible as water was found on the floor of the site (Figure 10c). The water pressure was measured at a pre-drilled borehole, and it was found to be around 4 bar. However, this pressure may be misleading since the measurement borehole was very short (few meters of length).

3.2.1.3 Elevator (depth: ~220m)

This site was located near the ventilation shafts and an elevator (Figure 11a). After visual inspection, no major water seepage areas were found. This site was also inconvenient for grouting due to the location of the elevator.

3.2.1.4 NASA0748 – Pump station (altitude unknown)

This site was in front of the pump station in the Äspö tunnel. The fractures could be noticed at a visual inspection and water seepage was clearly observed (Figure 11b-c). The water pressure was measured at the pump station wall, and it was found to be around 9 bar. However, this site was inconvenient for grouting due to the pump station location.

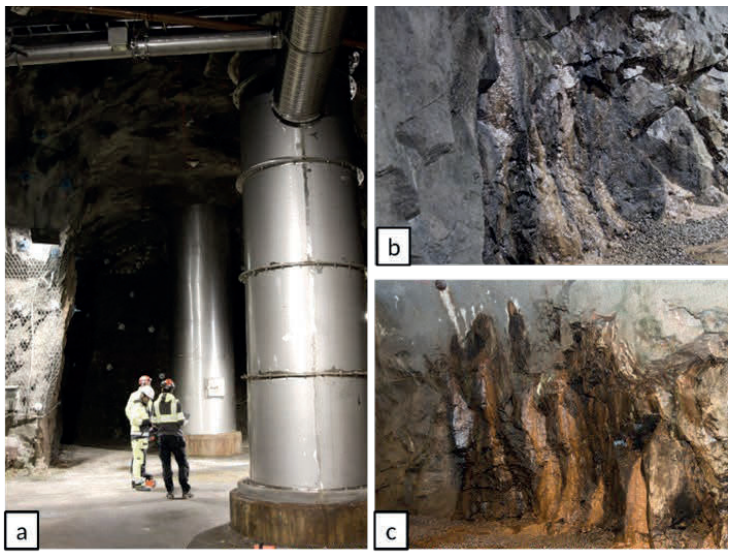

Figure 11. Two inspected sites a) elevator area with ventilation shafts b) site NASA 0748 with water ingress at the rock face c) site NASA 0748 also with water ingress

3.2.1.5 REDOX (TASR)

Another promising site was REDOX (Figure 12a) since it had been used for experiments concerning ground water analysis. The water pressure was measured at a pre-drilled borehole, and it was found to be around 5.5 bars. In addition, the boreholes were inspected using a fibreoptic camera and fractures were observed in the longitudinal and the transversal direction (Figure 12b).

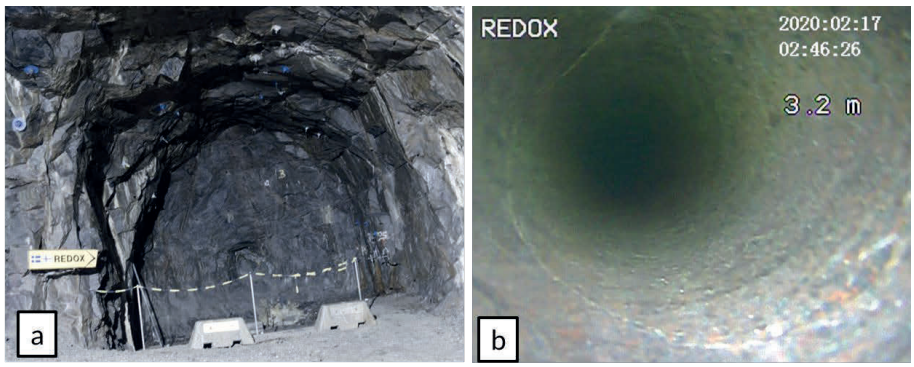

Figure 12 REDOX (TASR) site: a) overview of the site b) fractures in the borehole.

3.2.1.6 NASA 0408A

At this site (Figure 13a), no major fractures and water seepage were observed. It may be due to previous grouting experiments at this site in which fractures were filled using grout.

3.2.1.7 TASM

At this site (Figure 13b), water leakage was observed at the wall. The water pressure was measured in a pre-drilled borehole, and it was found to be around 5.5 bars. The very deep borehole (~45 m) was inspected using a fibreoptic camera and fractures were observed in the longitudinal and the transversal direction (Figure 13c).

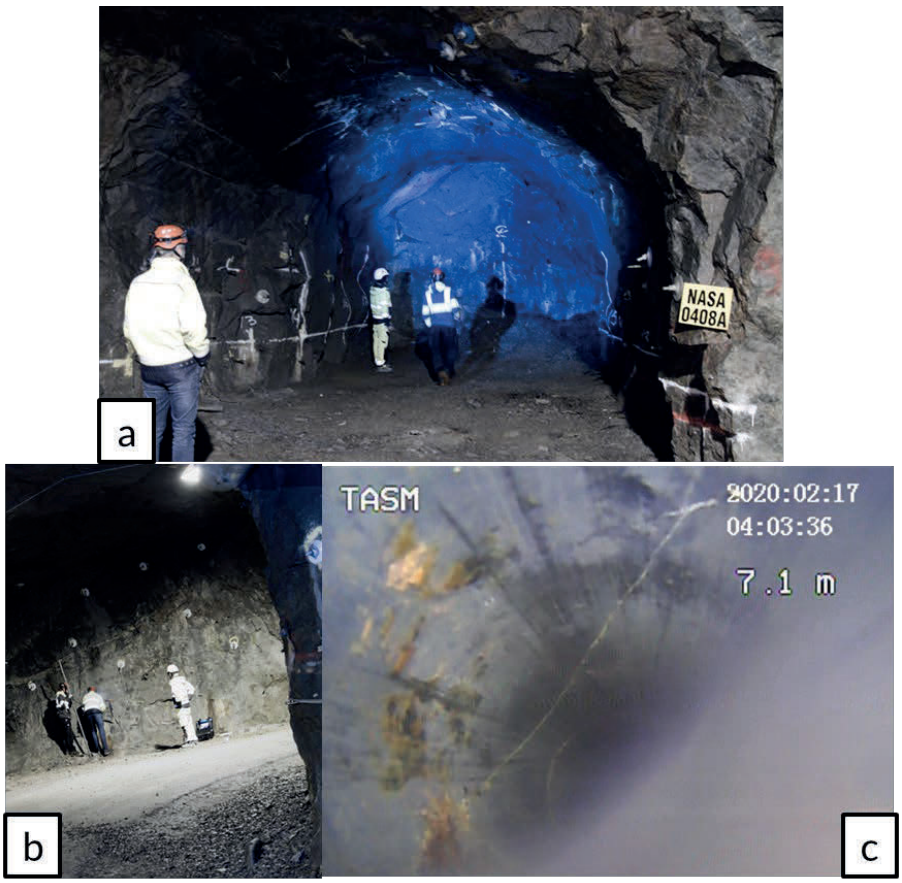

Figure 13. Inspected sites: a) NASA 0408A b) TASM site c) fractures in the borehole at the TASM site.

3.2.1.8 NASA 0249A (~30 m)

The site NASA0249A (Figure 14a) was located at a depth of ~30 m and it was the site nearest to the tunnel entrance. The rock wall at this site displayed multiple fractures wetted by the water seepage (Figure 14b), however no major leakage was observed which, however, may be due a low a ground water pressure at 30 m depth.

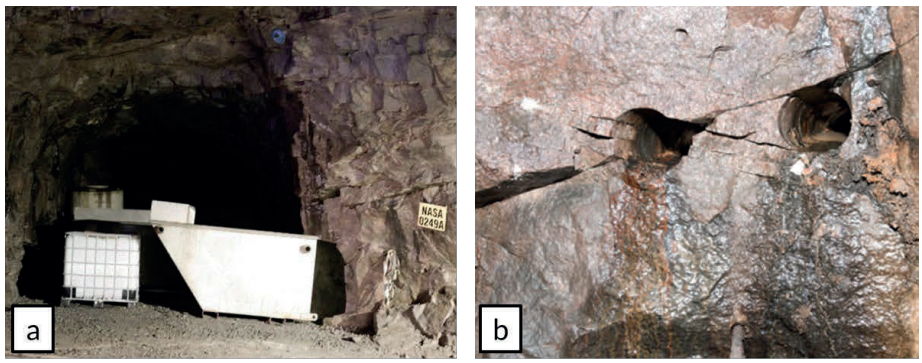

Figure 14 Inspected site: a) NASA 0249A site (b) fractures at the rock surface with the signs for water ingress.

3.2.2 Selection of the final site

Two final candidate sites were selected based on inspection results and geological data of the sites provided by Äspö HRL. Multiple factors were considered for the selection of the site.

- REDOX (Figure 12):
  - It showed good water ingress at previously drilled boreholes.
  - The pressure of water at previously drilled borehole was measured to be ~5 bar.
  - Multiple fractures were observed in the borehole.
  - The area was accessible for drilling and grouting.
  - Negative aspect – ground water analysis experiment was running at the site.
- NASA0249A (Figure 14):
  - This site was located at a small depth from the surface, so it may require only a low injection pressure.
  - Multiple fractures were observed on the rock surface.
  - The occurrence of the water ingress at the rock surface indicated that fractures could be connected (good connectivity) in the rock.
  - Access area was available for drilling and grouting.

After discussion with Äspö HRL, REDOX site was rejected because of the risk of disturbing the on-going ground water chemical analysis experiment. Thus, based on all above considerations, the NASA0249A site was selected for the field test experiments.

3.3 Drilling of boreholes

After selection of site – NASA0249A –the drilling contractor from Äspö HRL was hired. Based on the available space, 10 boreholes were drilled (Figure 15a). These 10 boreholes were evenly distributed along the tunnel walls: 5 boreholes on the right side and 5

boreholes on the left side. The height of the boreholes from the ground was ~1.5 m, so that packers (grout packers) could be conveniently packed in the boreholes. boreholes with a diameter of 56 mm and length of 10 were drilled. It was found that the inclination angle of drilling direction was partly limited by the drilling equipment, but it was still possible to alter it to some extent (upwards, horizontal, or downwards) to increase the probability to intersect rock fractures with the borehole (Figure 15b).

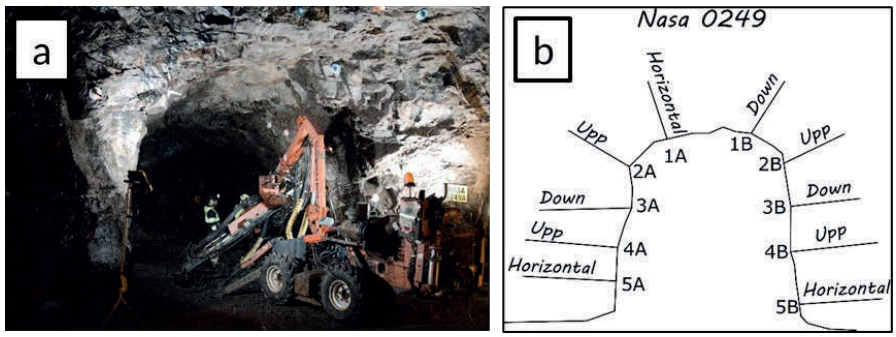

Figure 15 Drilling of boreholes at site in the Äspö tunnel: a) the drilling equipment at site (b) borehole plan with marked borehole inclination.

3.4 Design and development of distribution unit

3.4.1 Development of testing set up

To measure flow of the grout coming from distribution unit, appropriate flow meters were required. Two flowmeters (Batchflux 5500C, KROHNE Messtechnik GmbH, Germany) were acquired for the testing (Figure 16a). These flow meters are electromagnetic flowmeters (EMF) for rotary or linear filling machines. Due to the unique ceramic measuring tube, these flow meters had the best repeatability and long-term stability. One flow meter was assigned to measure flow in the dynamic injection regime, and another was assigned for the static injection. It was found that the flowmeters were not compatible with test data acquisition (DAQ) system that was available at the laboratory. The signal from the flowmeters resulted in a frequency output, whereas a voltage signal was required for the DAQ system. To resolve this problem, a special signal conversion device was constructed (Figure 16b), which consisted of two signal converters and a power supply.

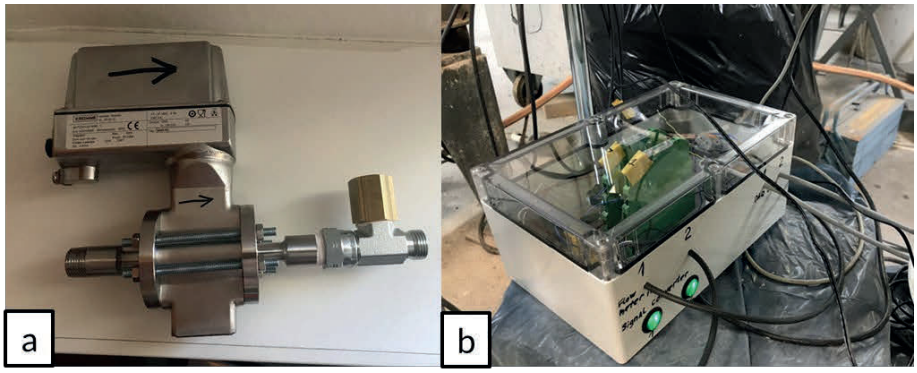

Figure 16. The flow meter set up: a) flowmeter Batchflux 5500C b) signal conversion device for converting frequency output of the flowmeters to voltage output for the DAQ system.

To check the reliability of flow measurement, the flow measuring and recording system were tested in the laboratory. A simple testing set was designed, in which tap water hoses were connected to the flowmeters (Figure 17) and the water from the flowmeter was directed to the bucket that hanged with the mass sensor. The mass change was recorded together with the flow rate (Figure 18). During this test, the tap valve was opened in 5 steps that gradually increased the flow rate of the water (Figure 18).

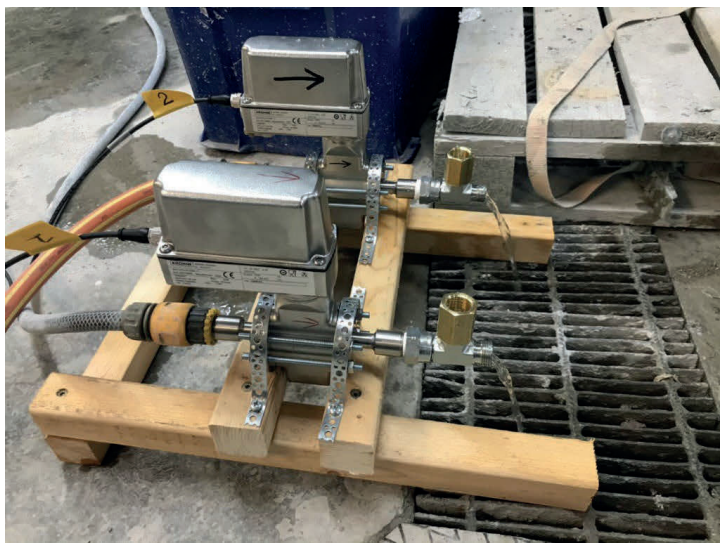

Figure 17. The flow meter connected to tap water hoses to test reliability of the signal conversion and the DAQ system.

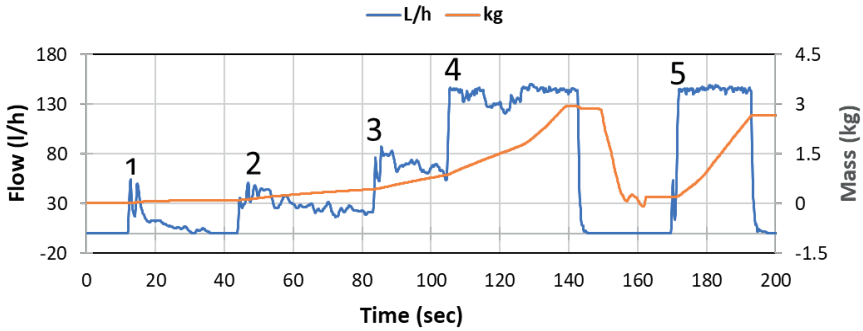

Figure 18. The flow rate of water measured by the flowmeter and the mass the water (in the collection bucket) measured by the mass sensor.

From the measured flow rate (measured by the flow meter), the mass of water was calculated and compared to mass of the water that was measured by the mass sensor within the same timeframe (Figure 19a-b-c). The packer difference between measured and calculated mass values in the flow measurement was considered as the error and is displayed in Figure 19. As seen from Figure 19a-b, at low flow rates (≤150 l/h), an insignificant difference was observed , whereas at high flow rates (≥ 150 l/h), the difference increased significantly and resulted in high errors (Figure 19c). After the analysis of the flow results, it was considered that signal conversion unit worked as intended. However, the flow meter displayed limited capability to measure flow rates ≥150 l/h. Thus, it was recommended that the flow rate of the grouting during the field test should be limited to less than 150 l/h.

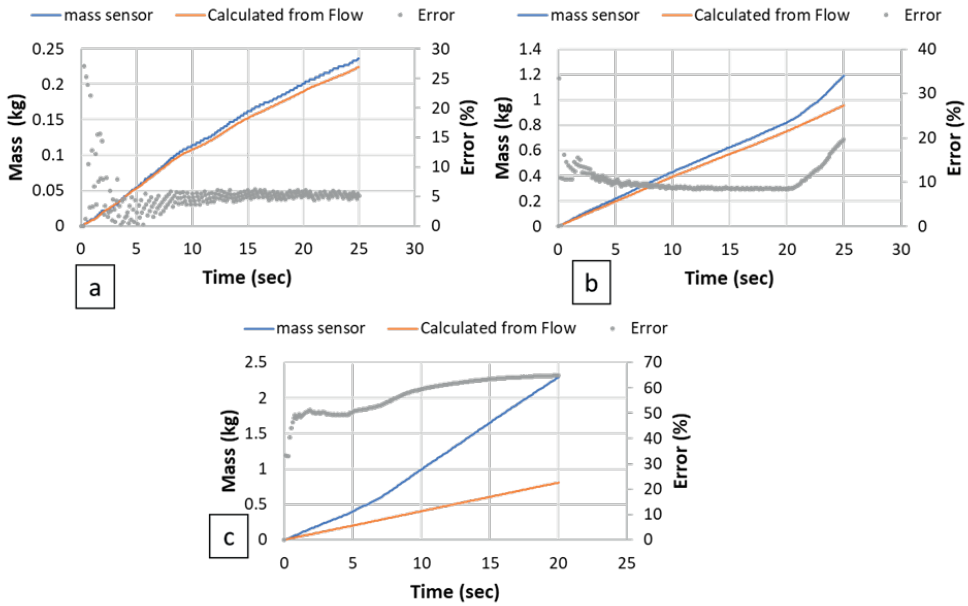

Figure 19. The measured mass of water and calculated mass of water. The dots show error values (difference between measured and calculated mass) at: a) average flow rate of 34 l/h; b) average flow rate of 171 l/h; c) average flow rate of 412 l/h

3.5 Experiments at NASA 0249A site

3.5.1 Ground water ingress test (hydro test I)

The first hydro test was performed in all 10 boreholes to measure the flow rate of the ingress of water in the boreholes. The test was performed as follows:

- The packers (Figure 20a) were installed in each borehole at least 2-3 days before the test started, to achieve good pressure recovery (pressure build up) in the borehole.
- The pressure logger was connected to the packer at the borehole. The logger was started a couple of minutes before the opening of the borehole to record the data every 5 sec.
- After this initial setup, each borehole was opened, and the flow was recorded for 30 minutes.
- During this period, the flow rate with the measuring vessel and times measured manually with a watch. Thereafter, the packers were applied to close the borehole and the pressure build-up was recorded.
- A minimum recovery time of 30 minutes was maintained (for some boreholes prolonged recovery time was needed).

3.5.2 Water injection test (hydro test II)

The Hydro test II was carried out according to recommendations of project work group. The test was performed to investigate possible connectivity of fractures between the boreholes. This test used gas (from a nitrogen gas bottle) to pressurize a water container (Figure 20b). During the test, the pressurized water was injected in the borehole at 10 bars. However, due to friction in the connection tubes and fractures in the boreholes, the actual pressure decreased and stayed at 4-5 bar during the water injection. After water was injected in one borehole, the pressure change was recorded in other 5 boreholes. In this way, 6 boreholes were tested.

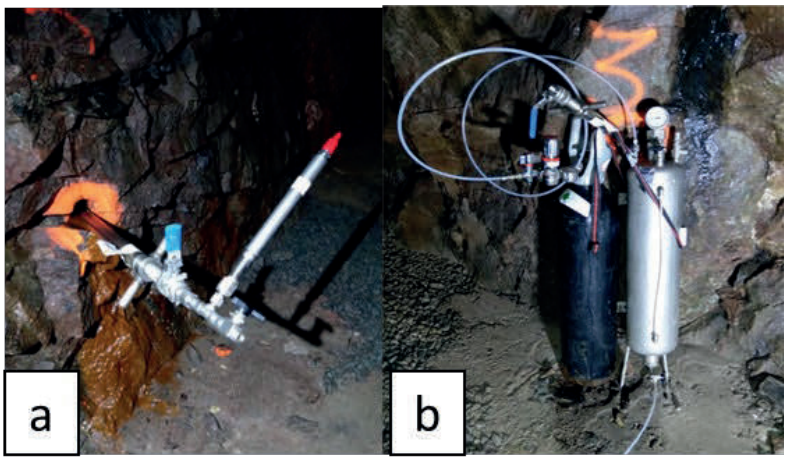

Figure 20. The hydro test II test setup a) packer with pressure gauge attachment b) nitrogen bottle, a pressure regulator, and a water container (capacity: 10 l).

3.5.3 Test setup for the field test at NASA0249A site

The test set up consisted of the injection system and the data acquisition system (Figure 21). The key components of the injection system were the injection pump (grout pump from BESAB), the distribution unit (developed at laboratory), the control box with pneumatic valves and the data acquisition system (DAQ). The DAQ module included flow meters, pressure meters and a PC (for data recording and visualization). Figure 21a shows schematic representation of the connection between all the components in the field test. The whole set up was operated as follows:

- The grout pressure was created with valves system V1 and V2.
- The valves V1 and V2 were controlled by valve control system.

- The flow rate of grout was measured by flowmeters F1 and F2, whereas the grout pressure was measured by pressure sensors P1 and P2.
- Signals from sensors were acquired by the DAQ module and recorded in real time with the PC.

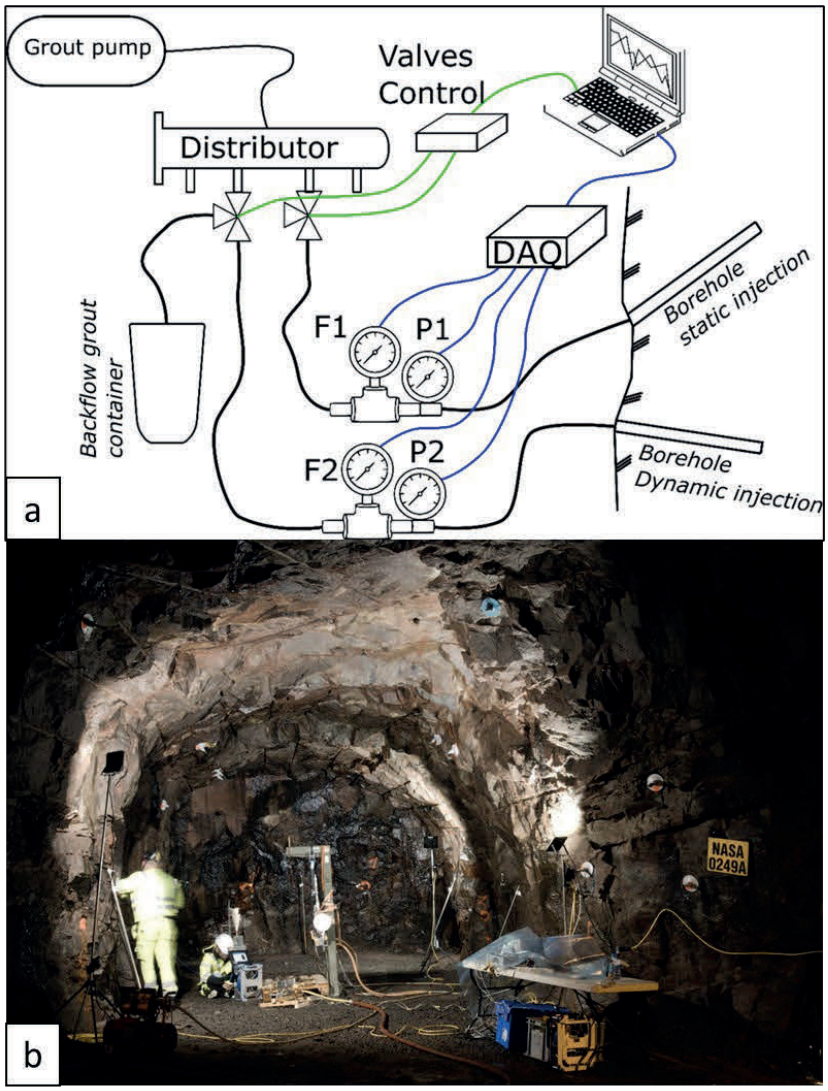

Figure 21 Experimental set up of the field-testing a) test setup schematics. (b) the final assembly for test setup in NASA 0249A.

As can be seen from Figure 21, the final field test setup deviated from the setup of the initial project description. In the project description, it was planned to inject 4 boreholes with dynamic injection simultaneously, however this plan was changed to two boreholes due to the multiple factors such as drilling budget, space limitation and expensive flow meters. Thus, it was decided to inject two boreholes simultaneously: one with dynamic and one with static injection. After discussion with project group, it was decided to leave out installation of inspection shafts due to budget limitation and difficulties in the evaluation in the limited space. After the initial setup, the grout pump was connected to the distribution unit using connecting hoses with 1 in diameter (Figure 21a).

To perform injection, the selection of appropriate individual boreholes was required. Thus, the 'ground water ingress flow rate' from hydro tests were used as benchmark for selecting injection boreholes and the boreholes were grouped in three pairs (Figure 22 and Table 2).

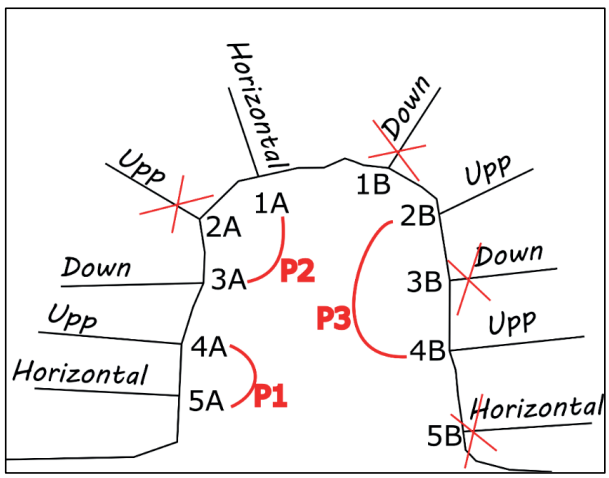

Figure 22 The pairs for the boreholes and initial sequence for the borehole injection.

Table 2. The grouping of pairs of boreholes based on ground water ingress flow rate in the boreholes.

Pair	Boreholes	Flow rate (l/min)	Injection type
P1	5A	1.32	*Dynamic*
	4A	0.72	Static
P2	1A	0.54	Static
	3A	0.34	*Dynamic*
P3	2B	0.14	*Dynamic*
	4B	0.12	Static

During the field test, the injection of grout was started according to the plan described in Figure 22. But during the injection of the pair P1 (Figure 23), possible interference of pressure pulses (from dynamic injection to static injection) was observed between the adjacent boreholes. Thus, during the experiment, it was decided to replan the injection sequence for the boreholes for the remaining pairs P1 and P2 (Figure 23 and Table 3). The pairs were redistributed in such a way that each pair consisted of opposite side boreholes to reduce the possible interference during injection. Also, it was decided to inject only one borehole at a time, starting with dynamic injection and continuing with the static injection.

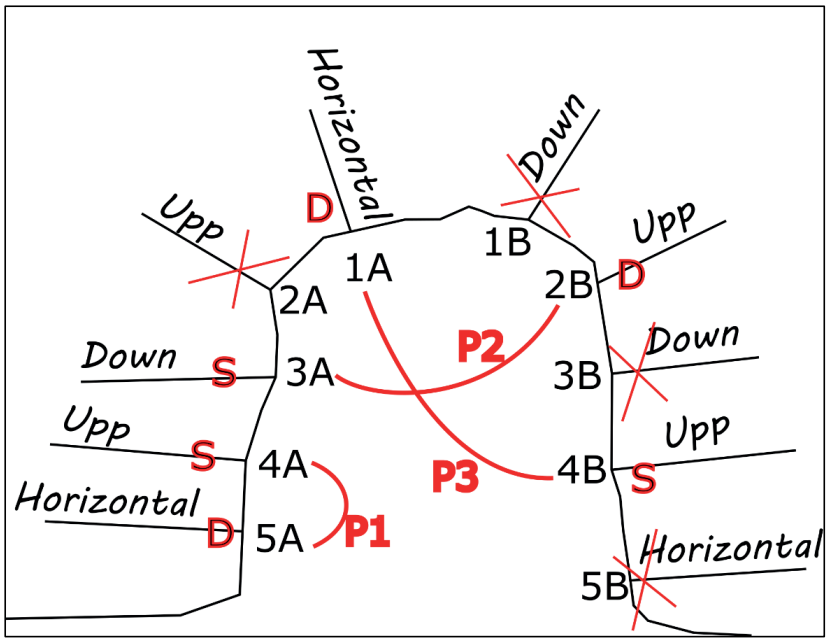

Figure 23. The updated test plan after performing injection tests on the P1 pair. The letter S stands for static injection and letter D for dynamic injection.

Table 3. The updated pairs of boreholes after injecting pair P1.

	Static Injection	Dynamic injection	Water test flow rate [l/min]
Pair 1	4A		0.72
		5A	1.32
Pair 2	3A		0.345
		2B	0.14
Pair 3	4B		0.12
		1A	0.54

3.6 Results

3.6.1 Water ingress test (Hydro test I)

The flow rate from the borehole was decided as benchmarking criteria for selection of the borehole for the field test. Based on water ingress results only 6 boreholes showed measurable water flow (Table 4) and was chosen for further testing (highlighted in green). The 4 boreholes were rejected due low flow rate (≤ 0.1 l/min) indicating less fractures in the borehole.

Table 4. Hydro test I results for all boreholes. Green and grey highlighting suggest high and low flow rate values respectively.

Name of borehole	Side in the tunnel	Direction	Pressure (kPa) in borehole	Flow rate (l/min) from borehole	Selection	Hydraulic conductivity (l/min) /(m^2)
5A	left	Horizontal	141	1.32	Yes	0.87
4A	left	Upward	135	0.72	Yes	0.48
1A	left	Horizontal	232	0.54	Yes	0.36
3A	left	Downward	120	0.345	Yes	0.23
2B	right	Upward	285	0.14	Yes	0.09
4B	right	Upward	227	0.12	Yes	0.08
1B	right	Downward	270	0.012	No	0.01
3B	right	Downward	270	0.0076	No	0.01
2A	left	Upward	110	0.005	No	0.00
5B	right	Horizontal	102	0.0017	No	0.00

3.6.2 Water injection for testing fracture interconnectivity between boreholes (Hydro test II)

Figure 24 s shows that possible interaction was observed between boreholes 5A and 4A (which was also found during grout injection). A similar indication of strong interference was also observed between boreholes 3A and 1A. In case of boreholes 2B and 1A, and 2B and 4B only minor interference was observed. To avoid interference affecting the results the testing protocol for boreholes 1A, 3A, 2B and 4B was redesigned to group the boreholes in appropriate injection pairs (Figure 23).

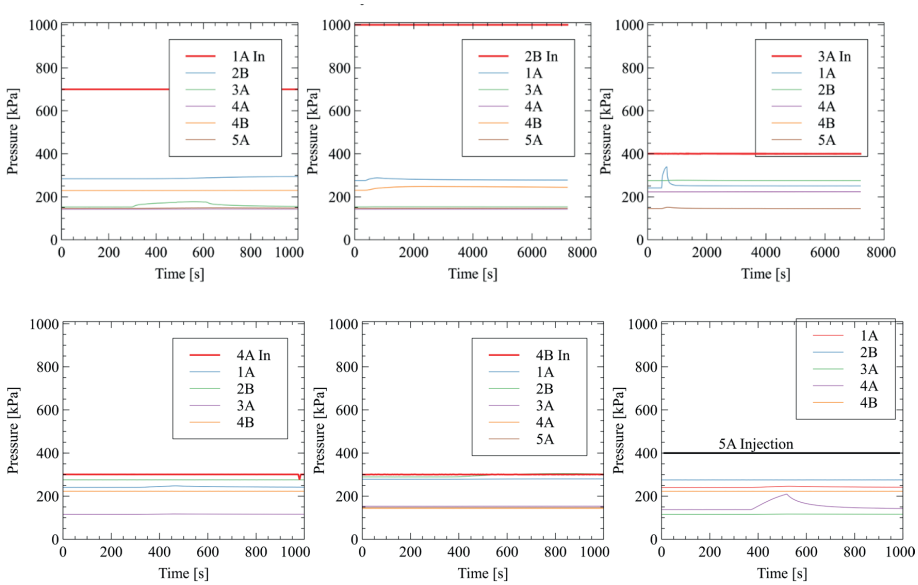

Figure 24. Pressure in the boreholes during Hydro test II. The injected borehole name marks as "In" and the thick line represents the water pressure at entrance of the injected borehole.

3.6.3 Boreholes inspection with camera.

Before the grout injection, the 6 selected boreholes were inspected using fiberoptic camera. The camera inspection revealed that fractures in the rocks were located at the beginning of the boreholes. Moreover, all boreholes consisted of fractures which were almost parallel to borehole drilling direction. Based on the camera inspection results, it was decided to insert packers at as close to the entrance as possible in the borehole, to avoid blocking of fractured areas close to the entrance of the boreholes.

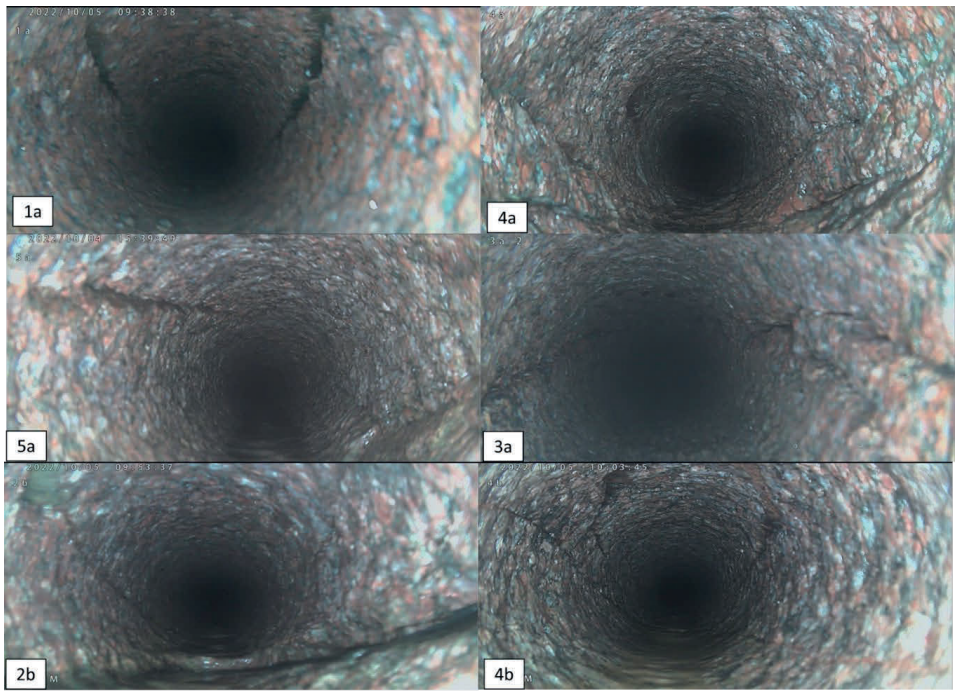

Figure 25. The borehole inspection and fractures in the borehole in the selected 6 boreholes.

3.6.4 Grout injection results

The injection results are given in the following sections. For more detailed information, the full-size graphs can be found in the appendix.

3.6.4.1 Pair P1 (5A-4A) injection results

Boreholes 5A and 4A were the first pair to tested, t and they were injected simultaneously. 5A was injected with the dynamic procedure and 4A with the static procedure. The grout injection lasted approximately 20 min, and therefore, the graphs are presented in two parts (for 5A, Figure 26 and for 4A Figure 27). During the injection process, there were technological stops (for mixing a new batch of grout h and emptying grout from the backflow container) and these stops can be clearly observed when grout pressure dropped to 0 and 2 bar.

As, it was observed from the values for 4A (Figure 27), the static pressure and flow was interrupted by pressure changes in the adjacent borehole 5A, which was also confirmed by the Hydro test II results (Figure 26). Also, it indicated that pressure interference was only marginally affected by the injection hose system, since during pressure drop in 5A, the injection valve was closed.

This prevented pressure drop in the grout from the distributor unit and in the static injection at the borehole 4A.

Nevertheless, the flow rate over time was not affected in neither boreholes, which showed that the boreholes had large apertures, and the grout flow was reached at the maximum limit for the flowmeters (see section 3.4.1). During injection of 5A part II (Figure 26 from time 350 sec), grout was injected efficiently using dynamic injection technique. At this point, the injection profile was modified by elongating injection time to 10 sec (from 4 and 6 sec) and by increasing the time period the backflow valve was open to obtain large pressure drops (see large pressure and grout flow rate drop at Figure 26). This action improved the injection pressure at the borehole entrance from a peak of 11 bar to a peak of 13 bar. Despite the pressure interference during static injection, a lower (1-2 bar) injection pressure in borehole 4A was observed compared to dynamic injection pressure at 5A.

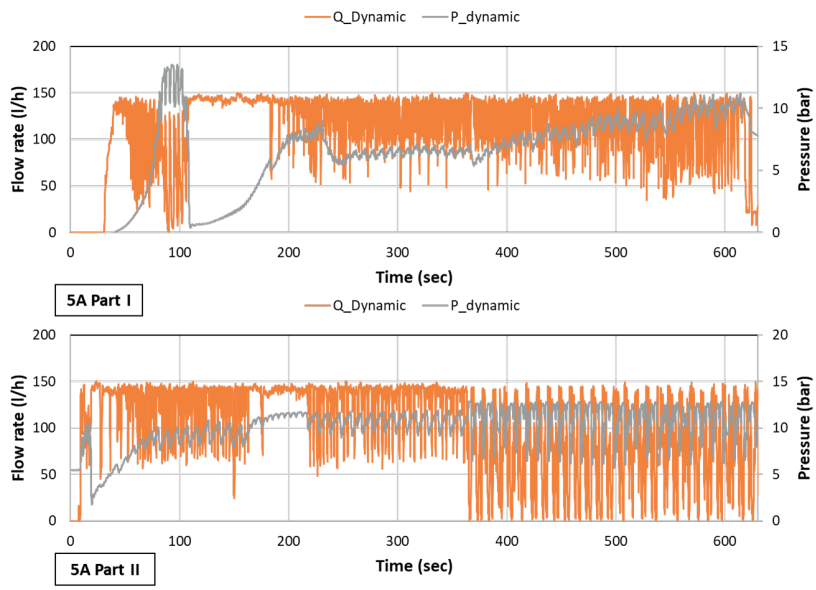

Figure 26. Dynamic injection in the borehole 5A Part I and Part II.

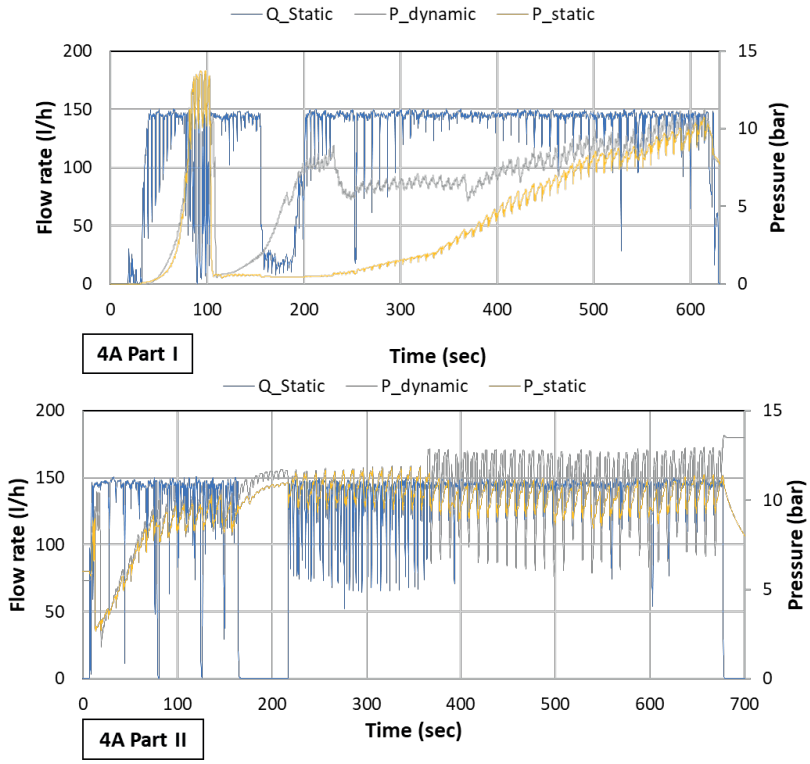

Figure 27. Static injection in borehole 4A Part I and Part II.

3.6.4.2 Pair P2 (3A-2B) injection results

Although all sensors were cleaned before starting the test, during dynamic injection at 2B, the pressure sensor showed indications of clogging with grout particles, since the pressure dropped to almost constant value of 1 bar (Figure 28). This clogging problem was difficult to resolve during ongoing test, thus it affected the results for dynamic injection in the pair P2. After removal of the clogging, the flow rate for each test was regulated manually using valves on the distributor unit. This helped to keep the maximum flow of grout below the flowmeter measuring limits.

During injection, it was observed that the flow rate at both boreholes did not decrease (other than by manual regulation), thus the test was stopped after ~20 minutes or after grout appeared from in the fractures on the rock surface. This indicated that the boreholes consisted of fractures with large apertures that resulted in a constant flow during the injection.

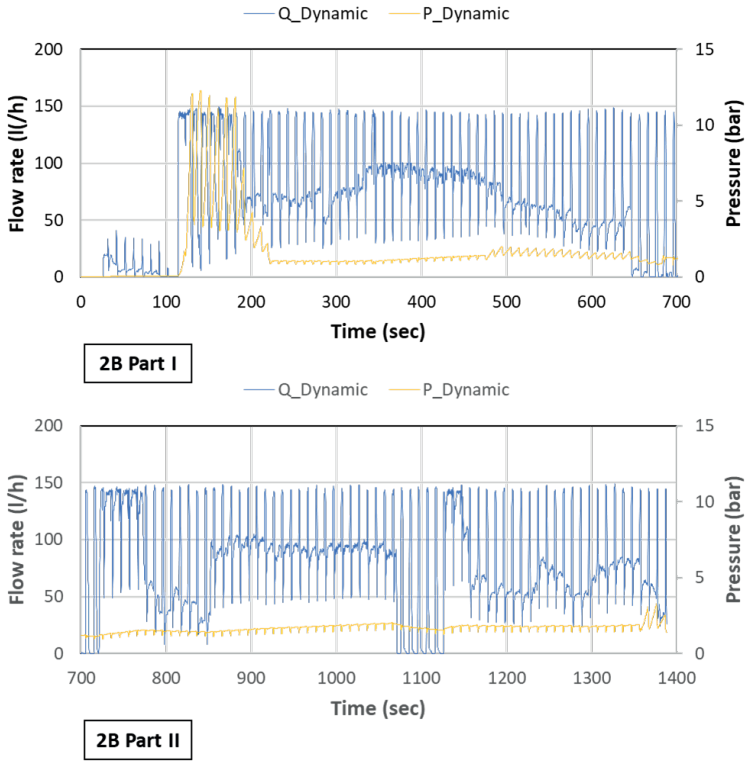

Figure 28. Dynamic injection in borehole 2B Part I and Part II.

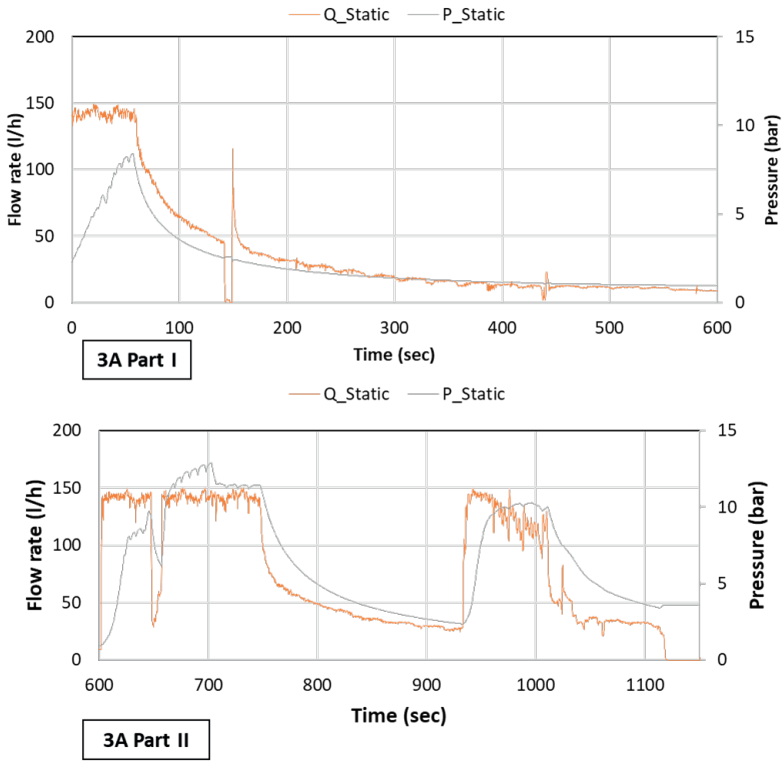

Figure 29. Static injection in borehole 3A Part I and Part II.

3.6.4.3 Pair P3 (1A-4B) injection results

In this test also, the pressure sensors were cleaned before starting the test. The pressure sensors were not clogged during testing and performed normally. The grout flow was controlled manually using valves on the distributor unit that continued to keep the flow rate below the measuring limits of the flow meter.

Figure 30 shows that the pressure was not reduced when the flow rate was dramatically lowered during dynamic injection in borehole 1A (refer the lowest point at flowrate in Figure 30). This is contrary to what happens in static injection at borehole 3A, in which the pressure dropped when the flow rate was decreased. These two boreholes were comparable since they exhibited almost similar flow of water in Hydro test I.

It was found during the injection that small pressure pulses were generated by the grout injection pump which was observed in the static injection (Figure 31), however they showed significantly lower frequency and amplitude (~1 bar) compared to the pulses generated by the dynamic injection.

Furthermore, during static injection, it was observed that the pressure in borehole 4B was not reduced along with the flow rate as it was reduced in static injection of borehole 3A. It was noted that borehole 4B showed the lowest water flow in Hydro test I, which indicates that 4B possibly contained less fractures or the fractures with smaller width. This may be the reason for the low dissipation of pressure during static injection. It was noted that borehole 2B displayed approximately the same flow rate as 4B in the hydro test. But due to clogging of the sensor during dynamic injection of 2B, it was not possible to conclude if dynamic injection helped to maintain (or increase) injection pressure in case of 2B (Figure 28) as it was observed for boreholes 5A and 1A.

Like pair P2, flow was not reduced in the pair P3 (other than manually reduced by controlling valves), thus the grout injection was stopped when grout leaked out from fractures at the rock surface.

As mentioned previously, the dynamic injection pressure was created with a grout backflow valve which resulted in a large quantity of backflow grout directed to the container (Figure 30 at 650-950 sec with visible longer flow peaks and lowest pressure drop to 2 bars). The open time for the back flow valve was altered from 0.25 s to 0.5 s which allowed to regulate the minimum pressure value at which pressure dropped during dynamic injection. During the first injection (pair 1), this backflow grout was discarded, but later on it was poured back into grout pump. During this time, int was necessary to pause the test. This problem could easily be solved by the use of an extra hose which could redirect the backflow grout so that it is returned to the mixer of the injection pump.

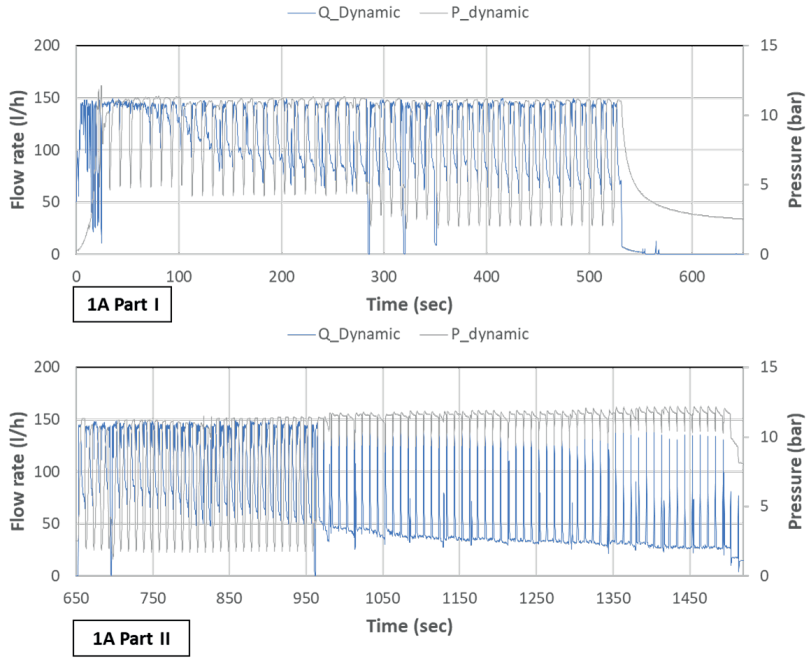

Figure 30. Dynamic injection in borehole 1A Part I and Part II.

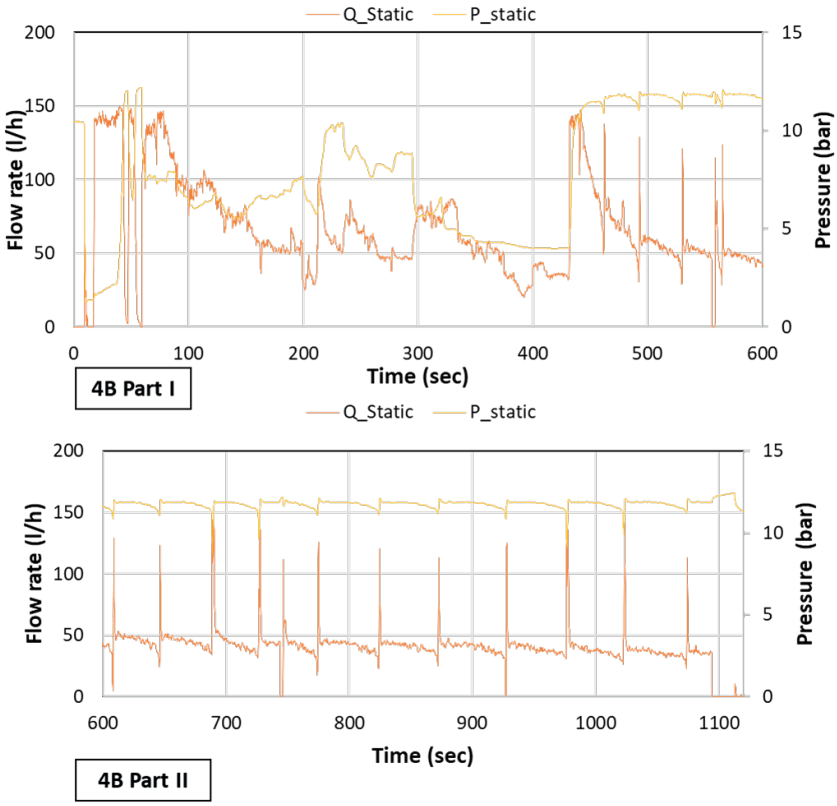

Figure 31. Static and dynamic injection in borehole 4B Part I and Part II.

4. CONCLUSION

The laboratory tests indicated that the grout injection rate under dynamic pressure conditions increased compared to under static pressure injection. Moreover, the grout penetrability in 60 µm and 70 µm apertures showed a steady flow rate under dynamic injection, compared to almost no flow during static pressure injection. In practical applications, this would help to improve penetrability of standard cement-based grouts that can reduce risk of water leakage and the need for chemical grouting. Moreover, the concept of a laboratory rig injection pressure control can easily be adapted to practical applications and can be connected to the existing injection pumps without major changes.

Moreover, field test results indicate that the dynamic injection helped to maintain maximum injection pressure at low flow rates. The dynamic injection approach even increased the injection pressure, when the injection period was elongated from 4 sec to 10 sec, and the pressure release period increased from 0.25 sec to 0.5 sec.

For boreholes with possible large apertures (based on Hydro test I flow results), the static injection pressure was reduced along with the flow rate reduction. This indicates that that in the field test the dynamic injection approach was not sensitive to changes in the flow rate and maintained a high pressure in the injection grout.

It was noted that, in general, grout in the field test displayed high flow rates. It was therefore not possible to be monitored by the flowmeters used in the test when an industrial injection pump operated at its nominal flow rate capacity. The flow meters in the test operated at over-flow conditions on some occasions due to the high flow rate of the industrial grout pump, and therefore it was impossible to capture reliable data at high flow rates (> 150 l/min). Moreover, it was not possible to relate the grout flow rate to water flow rate from Hydro test I, as was anticipated in the preparation stage of field test.

During the field test, the backflow pulses during dynamic injection were found to generate unexpected overflow peaks. This issue was difficult to predict during planning and laboratory, tests since there was no previous experience with monitoring dynamic injection under field conditions.

During dynamic injection, it was observed that the efficiency of the dynamic injection process could be increased, if the back flow grout (from the dynamic pressure control valve) could be redirected towards the grout pump. Also, the experience from pressure recording under field conditions showed that it would be helpful to use a minimum two pressure sensors instead of one, which would decrease the probability of data loss due to clogging of the single pressure sensor.

During this project, experiences was gathered in combining an experimental apparatus with an industrial injection system along with a laboratory sensor system applied under field conditions. This experience is valuable for future testing of dynamic injection in the field, where it could be efficiently used, simultaneously injecting multiple boreholes (20-30 borehole).

If the field tests could be performed on multiple boreholes, it would increase the possibility to compare dynamic and static injection, which are now restricted due to large variation of fractures in real rocks.

With multiple borehole testing, dynamic injection parameters could be recorded during differing parameters, such as injection peak duration, the backflow valve opening duration, injection peak pressure, varying lowest injection pressure. This would help to identify an optimum injection regime with respect to the hydraulic aperture of the borehole.

The test setup could be improved based on the field test experience. In future field test, the problem with measurements of large flow rates at injection could be solved by using two flowmeters with different measurement intervals (one for small flow rates and another for large flow rates) in serial connection. Also, the small size (1/2 in to 1/3 in instead of 1 in) hoses could be used to connect the grout pump, distribution unit, flow meters and boreholes for better control of the flow.

5. ACKNOWLEDGEMENT

This project has received funding from Bergteknisk Forskning Foundation (BeFo, the Swedish Building Industry Development Fund (SBUF) and RISE. We would like to give acknowledgement to project working group and the reference group. In addition, we appreciate the active participation from Ali Nejad Ghafar, Urs Mueller, Johan Gunnarsson and Ida Gabrielsson.

6. REFERENCES

Draganović, A., & Stille, H. Filtration and penetrability of cement-based grout: Study performed with a short slot. Tunnelling and underground space technology, 26(2011), 548-559. doi:10.1016/j.tust.2011.02.007.

Nobuto, J., Kobayashi, S., Nishigaki, M., Mikake, S., & Sato, T. (2008). Prevention of clogging phenomenon with high-grouting pressure. Doboku Gakkai Ronbunshu, C (CD-ROM), 64 (2008), 813-832. doi:10.2208/jscejc.64.813.

Pusch, R., Erlström, M., & Börgesson, L. (1985). Sealing of Rock Fractures A Survey of Potentially Useful Methods and Substances (Technical Report 85-17). Swedish Nuclear Fuel and Waste Management Co (SKB), Stockholm, Sweden, (1985).

Mohammed, M. H., Pusch, R., & Knutsson, S. Study of cement-grout penetration into fractures under static and oscillatory conditions. Tunnelling and Underground Space Technology, 45 (2015), 10-19. doi:10.1016/j.tust.2014.08.003.

Ghafar, A. N., Draganovic, A. & Larsson, S. (2015) An experimental study of the influence of dynamic pressure on improving grout penetrability. BeFo report 149, Stockholm, Sweden.

Ghafar, A. N., Draganovic, A. & Larsson, S. (2017) An experimental study to measure grout penetrability, improve the grout spread, and evaluate the Real Time Grouting Control theory. BeFo report 181, Stockholm, Sweden

Ghafar, A. N., Draganovic, A. & Larsson, S. (2019) Development of dynamic grouting, stage 1 / Utveckling av dynamisk injektering, etapp 1 BeFo report 197, Stockholm, Sweden

Ghafar, A. N., Mentesidis, A., Draganovic, A., & Larsson, S. (2016). An experimental approach to the development of dynamic pressure to improve grout spread. Rock Mechanics and Rock Engineering, 49 (2016), 3709-3721. doi:10.1007/s00603-016-1020-2.

Ghafar, A. N., Sadrizadeh, S., Draganovic, A., Johansson, F., Håkansson, U., & Larsson, S. Application of Low-Frequency Rectangular Pressure Impulse in Rock Grouting. Grouting 2017: Grouting, Drilling, and Verification. ASCE Geotechnical Special Publication, 288 (2017), 104-113. doi:10. 1061/9780784480793.010.

Standard SS-EN 14497:2004/AC:2006, Products and systems for the protection and repair of concrete structures - Test methods - Determination of the filtration stability. British Standards Institution. (2006).

Ulriksen, P. (2020) Dynamic Grouting Using Feedback Resonance, Square Wave excitation and the Water Hammer Phenomena BeFo report 207, Stockholm, Sweden.

7. APPENDIX

5A-4A test pair

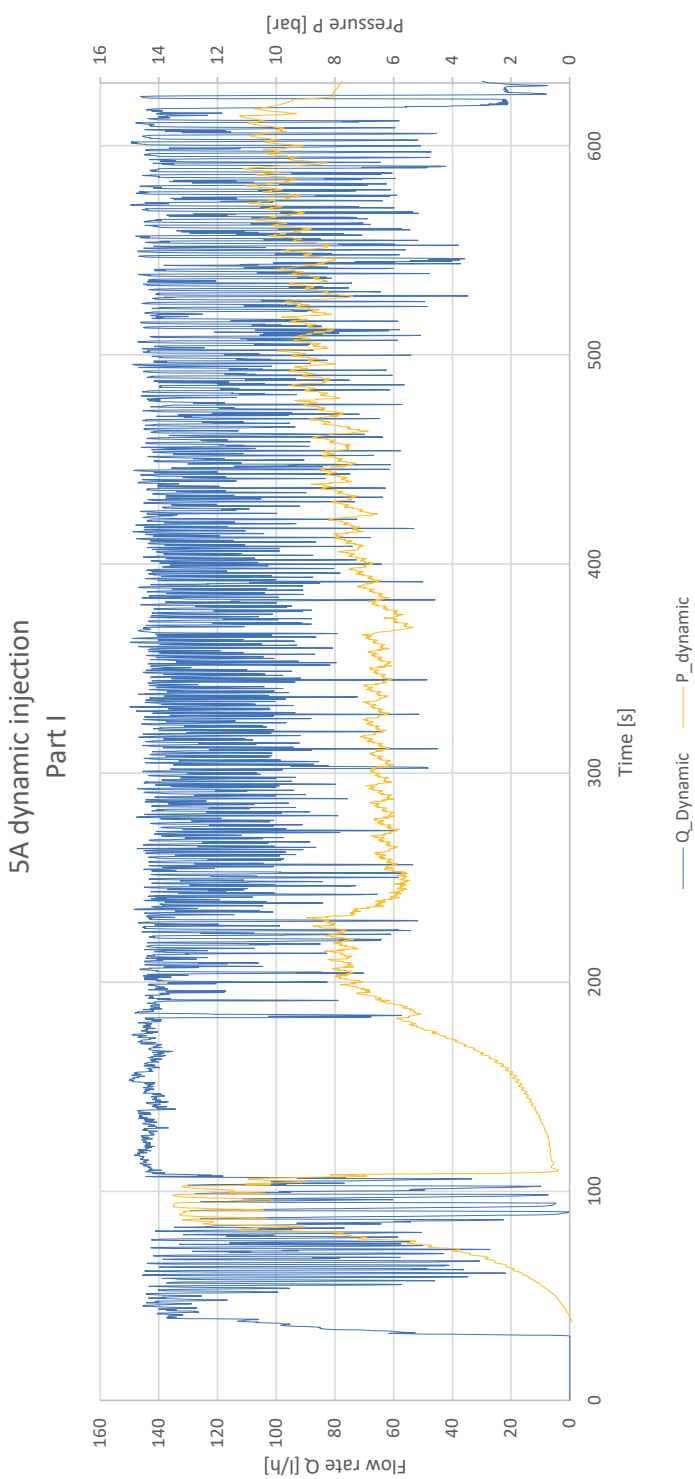

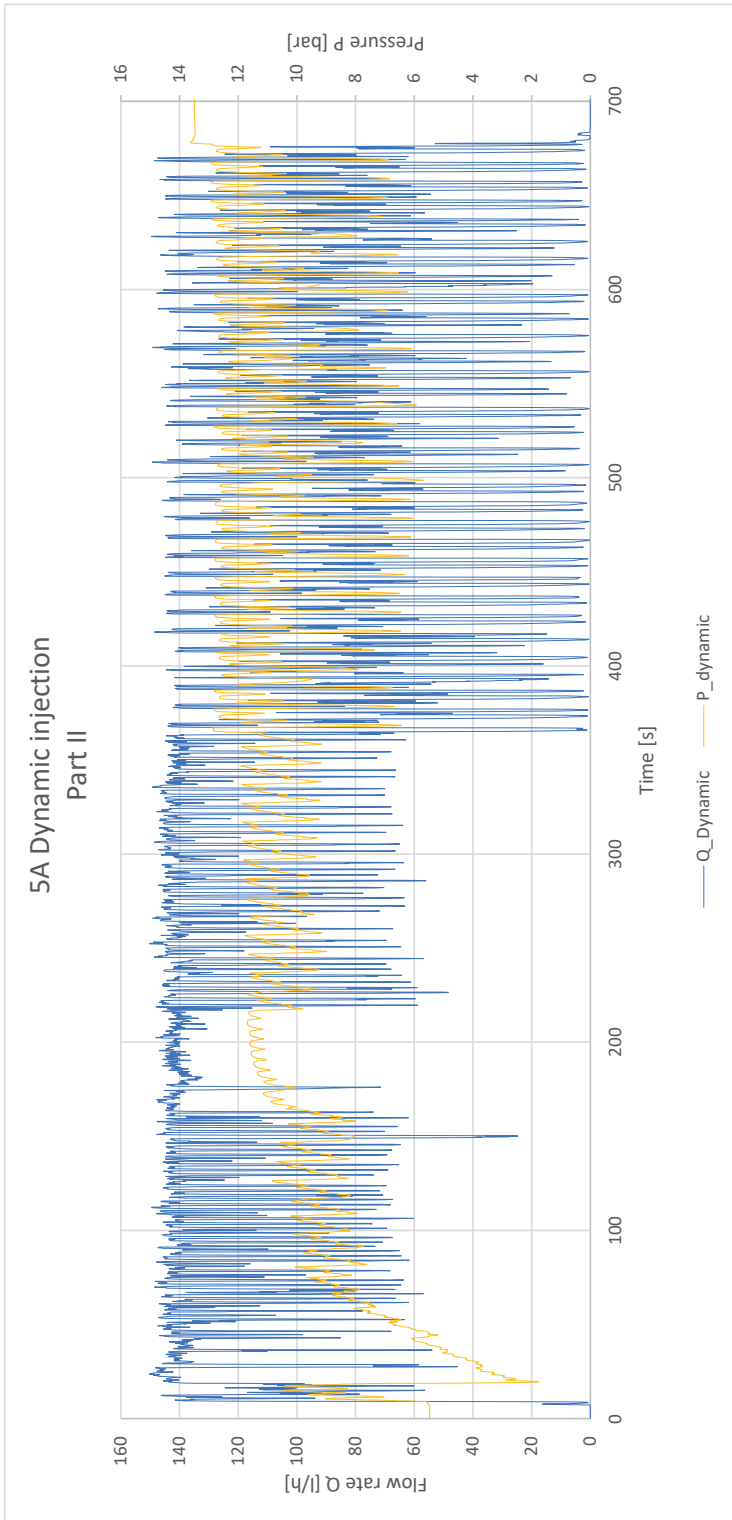
5A Dynamic injection
Part II
Flow rate Q [l/h]
Pressure P [bar]
Time [s]
Q_Dynamic
P_dynamic
0
20
40
60
80
100
120
140
160
0
2
4
6
8
10
12
14
16
0
100
200
300
400
500
600
700

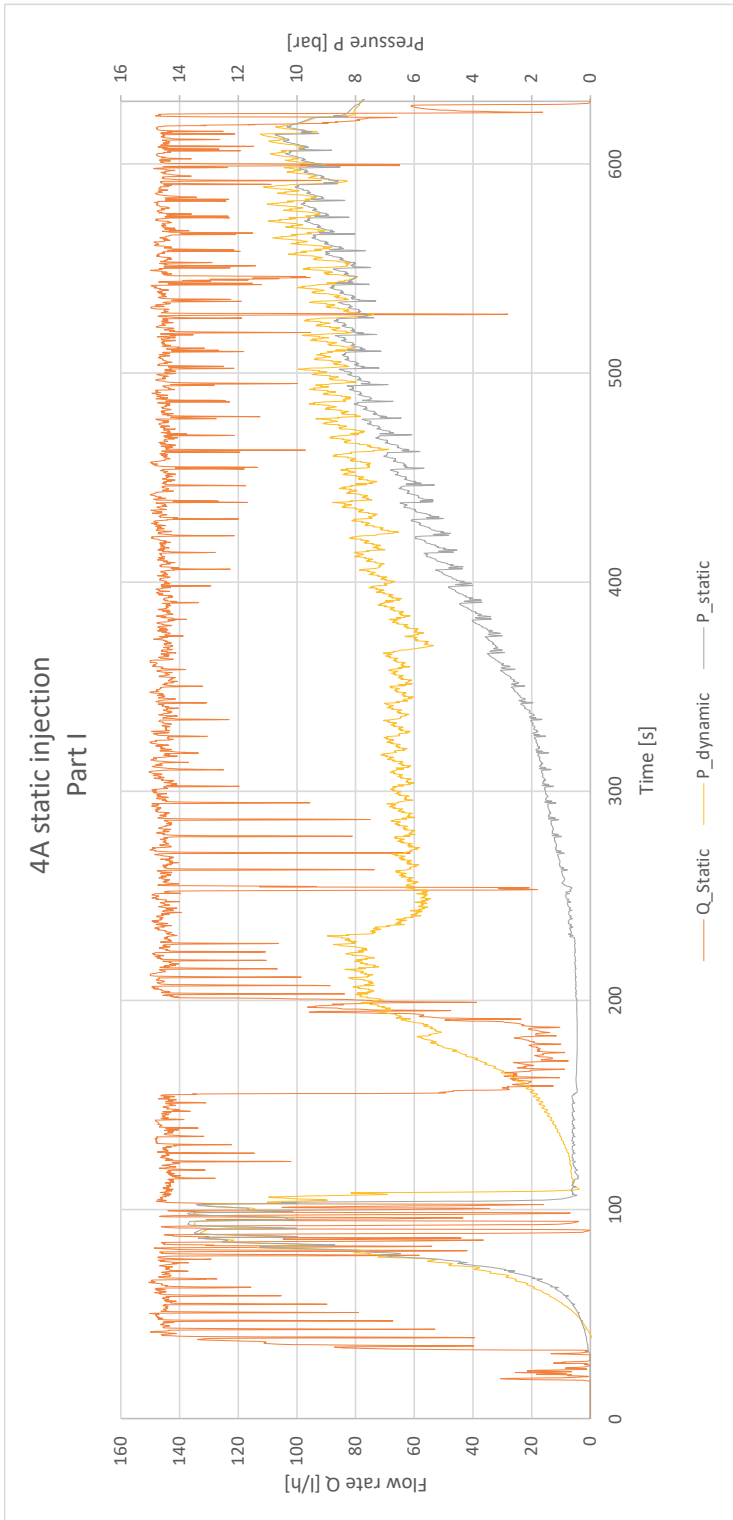
4A static injection
Part I
Flow rate Q [l/h]
Pressure P [bar]
Time [s]
Q_Static
P_dynamic
P_static
0
20
40
60
80
100
120
140
160
0
2
4
6
8
10
12
14
16
0
100
200
300
400
500
600

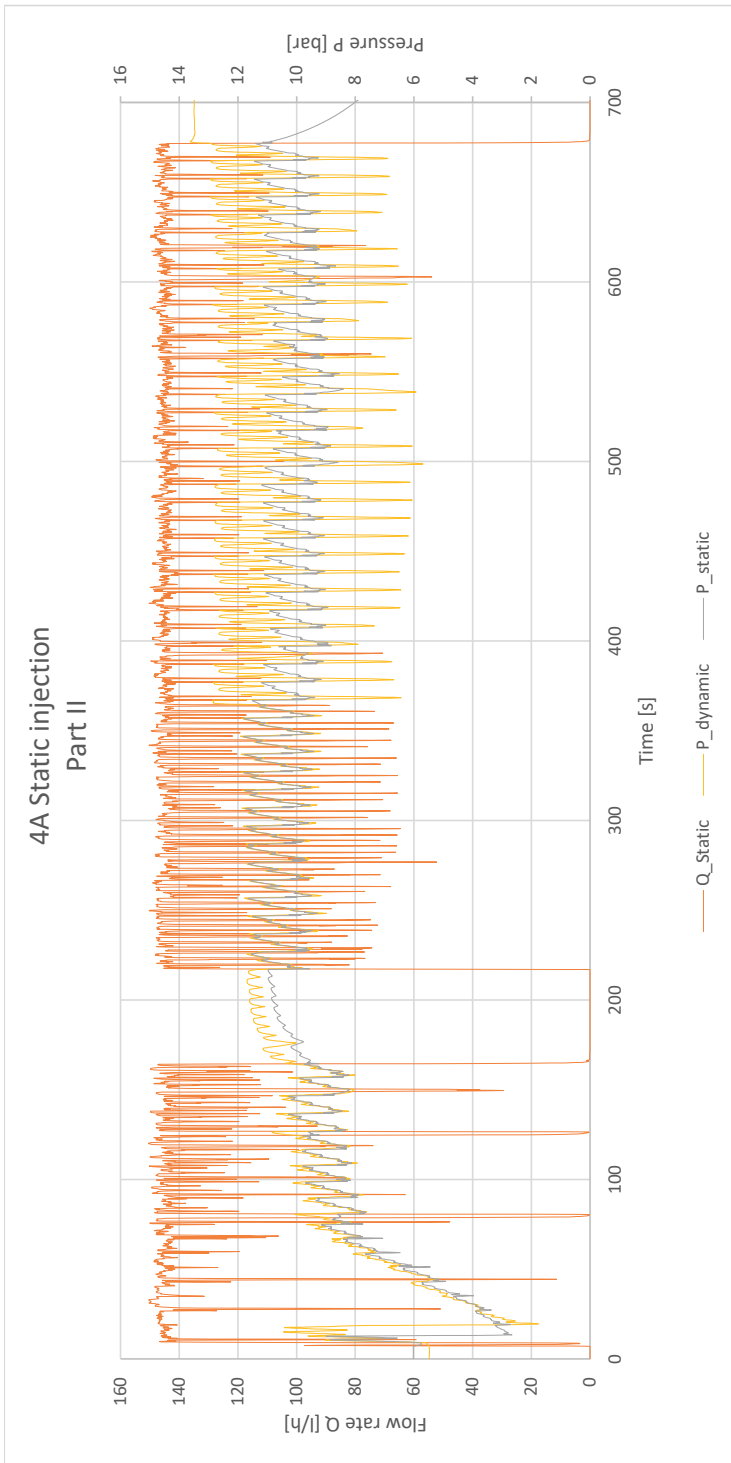
4A Static injection
Part II
Flow rate Q [l/h]
Pressure P [bar]
Time [s]
Q_Static
P_dynamic
P_static
0
20
40
60
80
100
120
140
160
0
2
4
6
8
10
12
14
16
0
100
200
300
400
500
600
700

7.2 3A–2B test pair

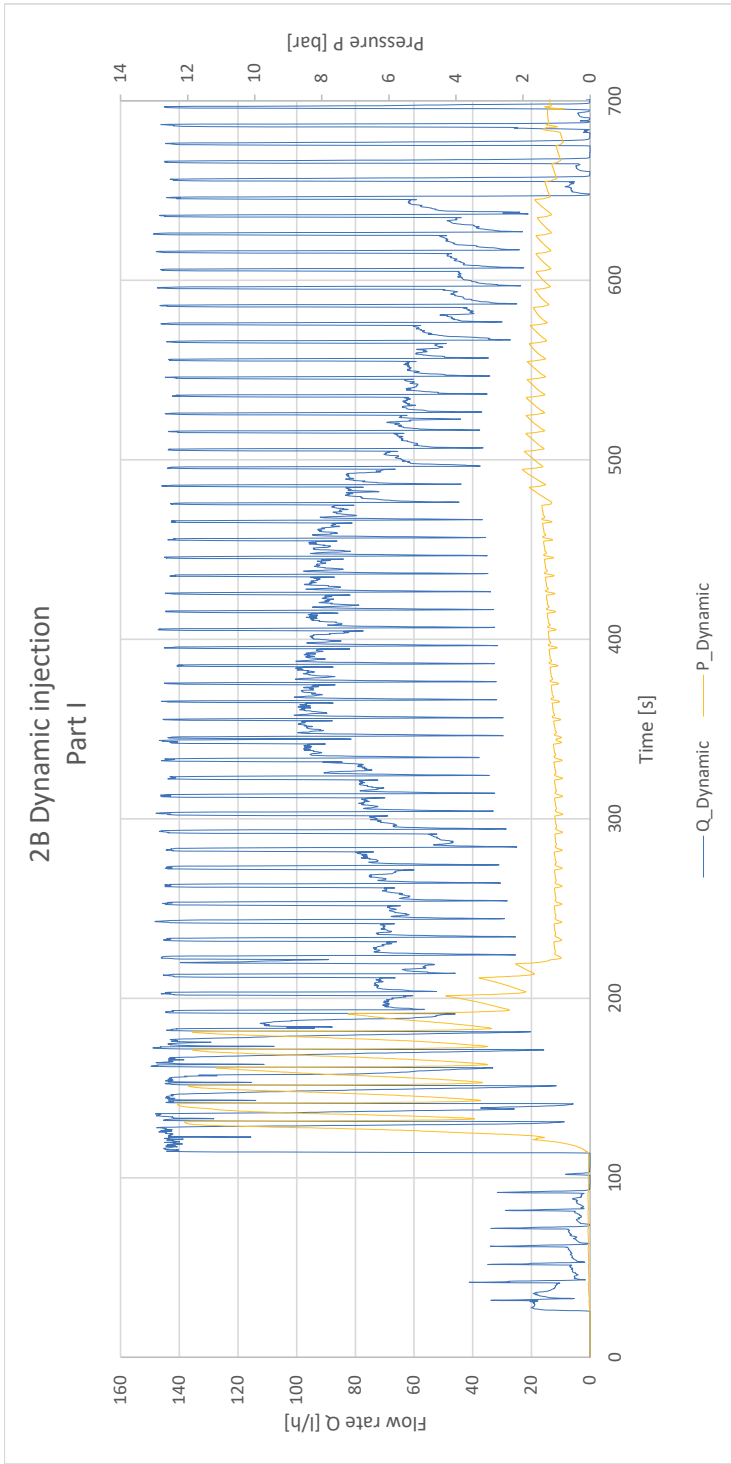

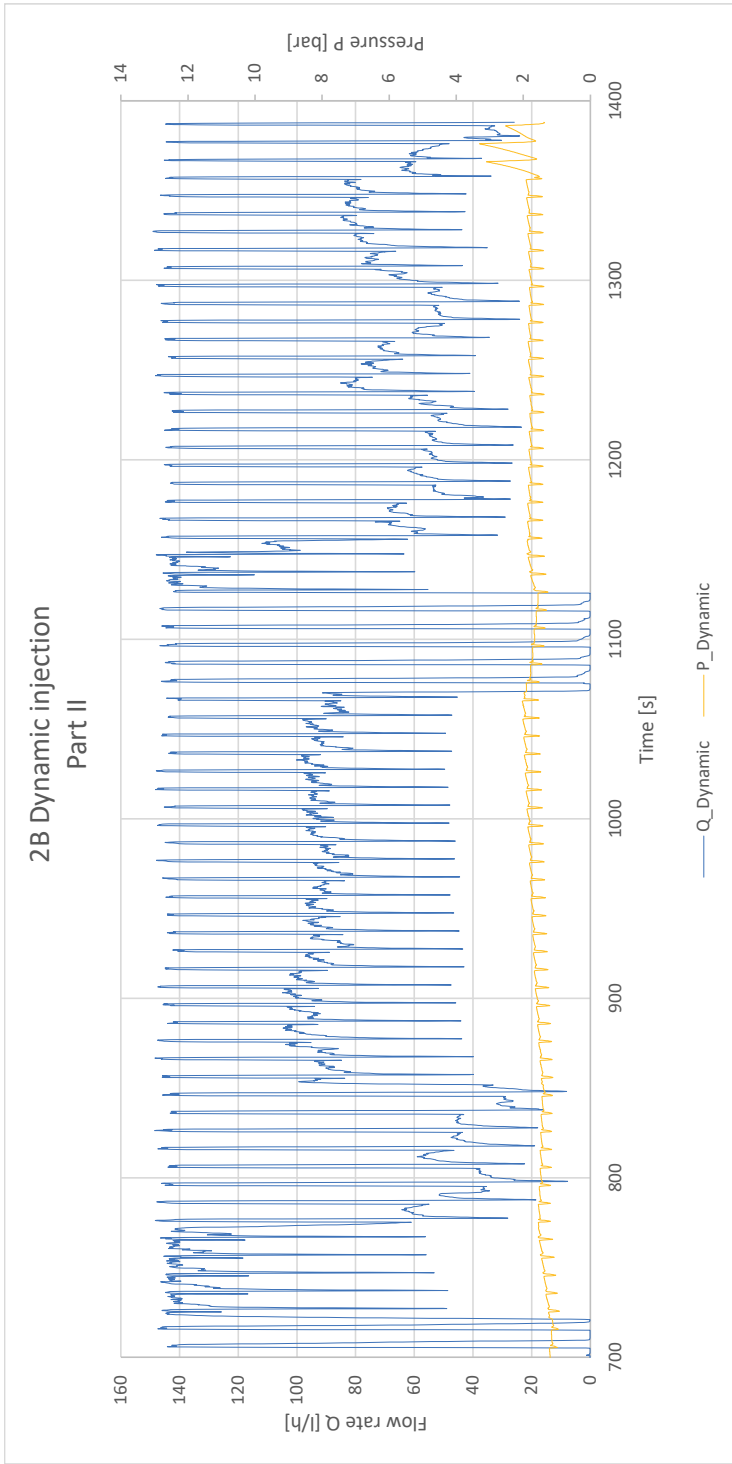
2B Dynamic injection
Part II
Flow rate Q [l/h]
Pressure P [bar]
Time [s]
Q_Dynamic
P_Dynamic
0
20
40
60
80
100
120
140
160
0
2
4
6
8
10
12
14
700
800
900
1000
1100
1200
1300
1400

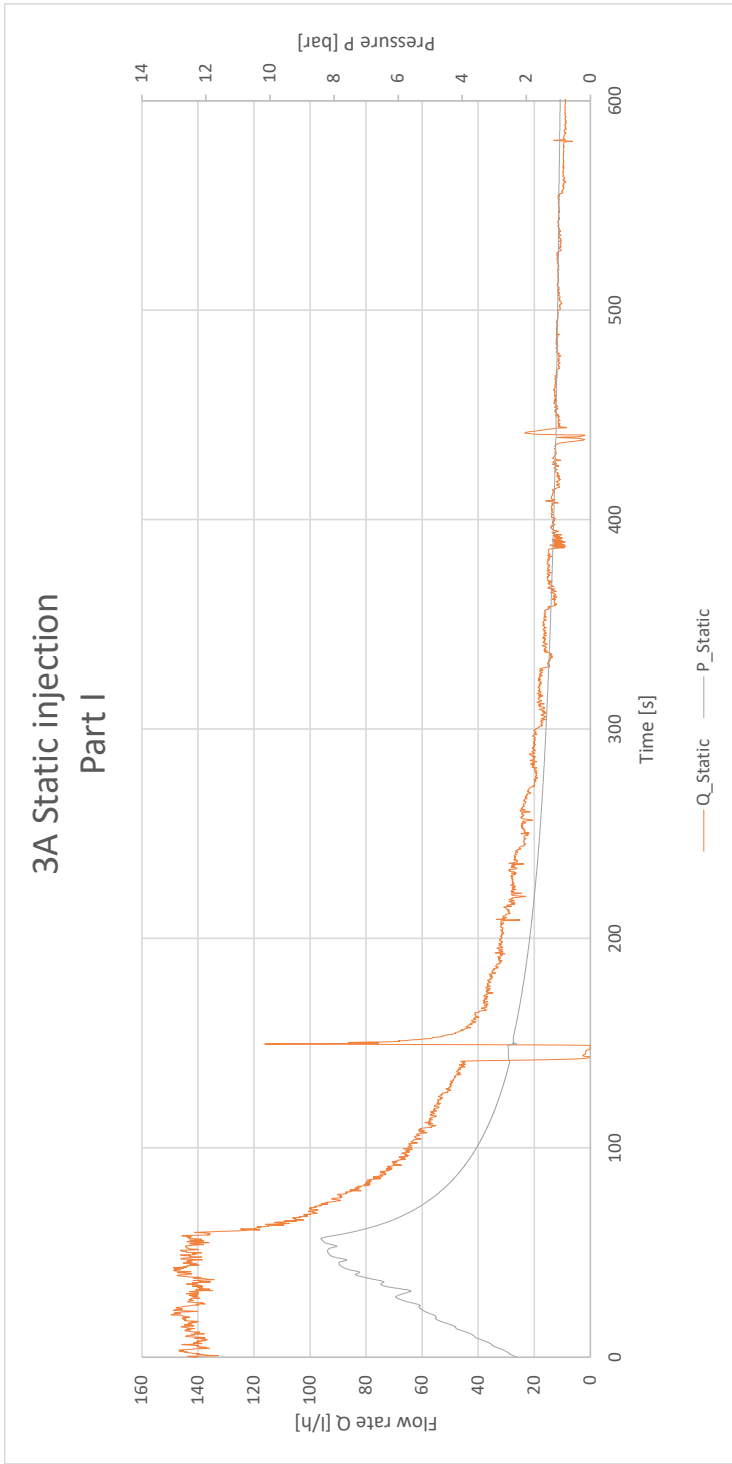
3A Static injection
Part I
Flow rate Q [l/h]
Pressure P [bar]
Time [s]
Q_Static
P_Static
0
20
40
60
80
100
120
140
160
0
2
4
6
8
10
12
14
0
100
200
300
400
500
600

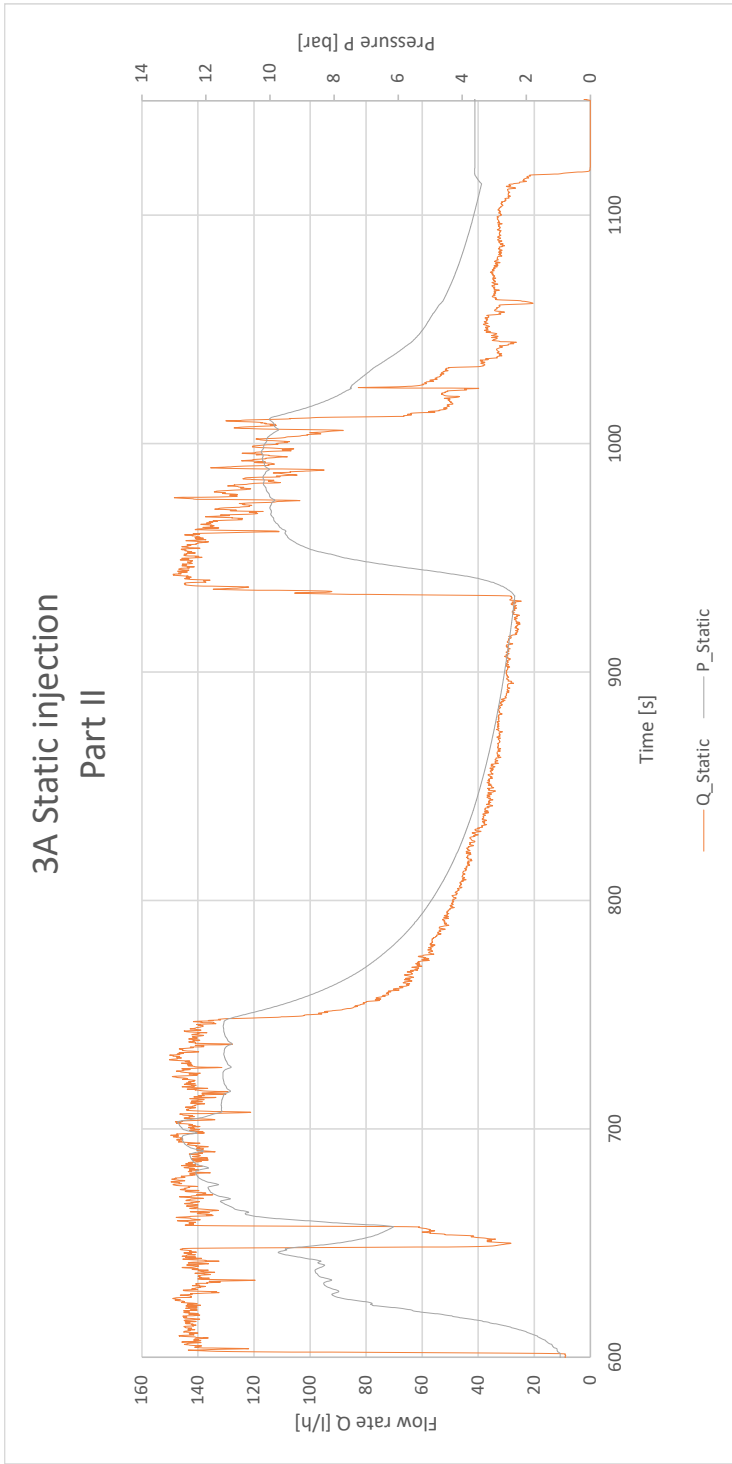
3A Static injection
Part II
Flow rate Q [l/h]
Pressure P [bar]
Time [s]
Q_Static
P_Static
0
20
40
60
80
100
120
140
160
0
2
4
6
8
10
12
14
600
700
800
900
1000
1100

7.3 1A-4B test pair

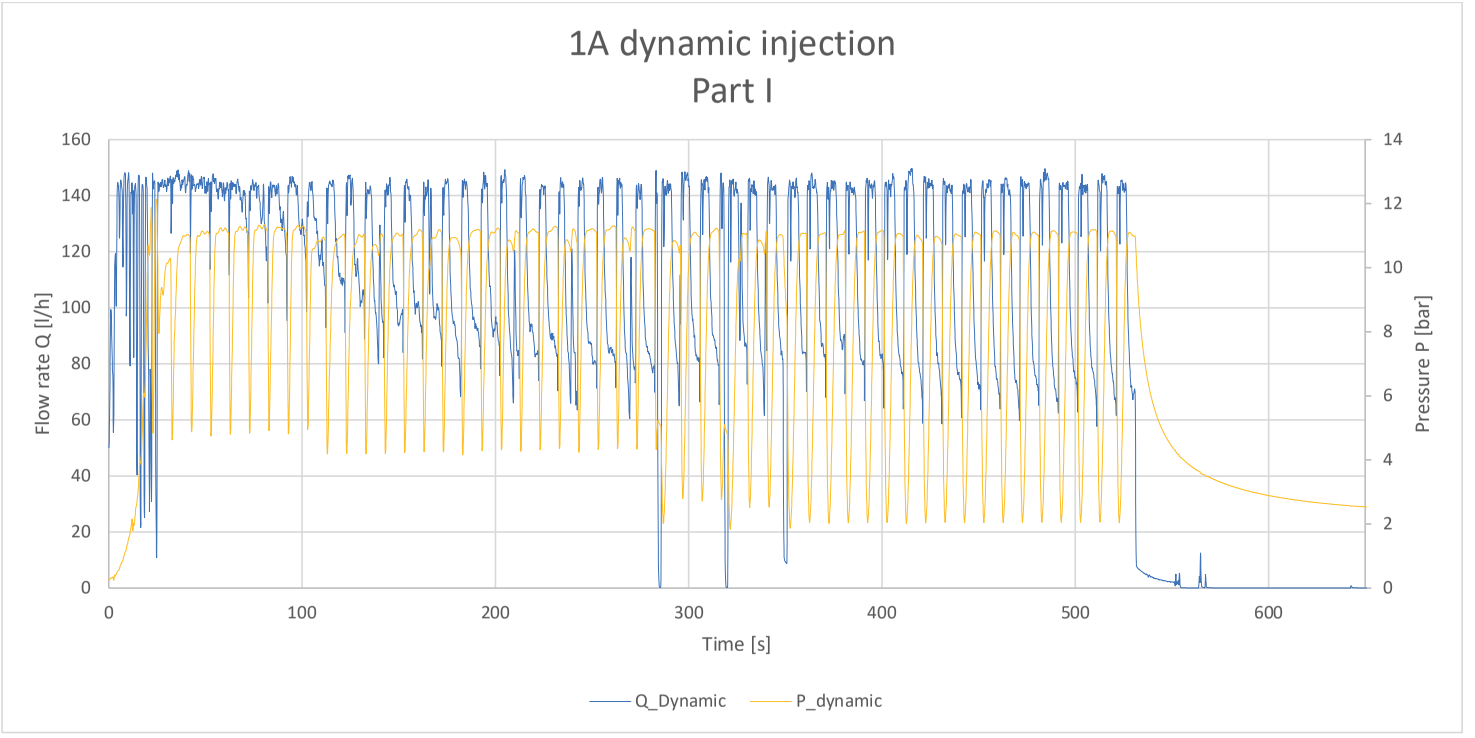

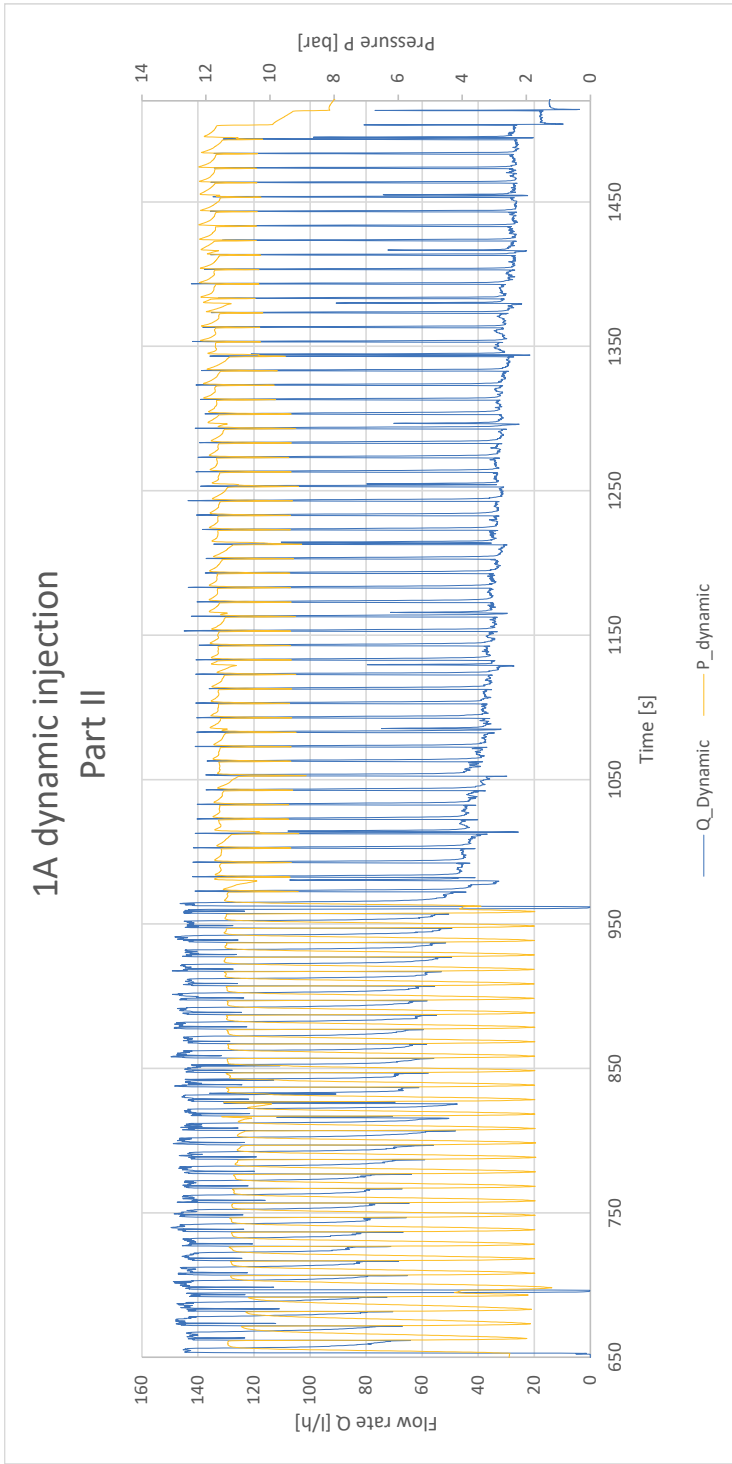
1A dynamic injection
Part II
Flow rate Q [l/h]
Pressure P [bar]
Time [s]
Q_Dynamic
P_dynamic
0
20
40
60
80
100
120
140
160
0
2
4
6
8
10
12
14
650
750
850
950
1050
1150
1250
1350
1450

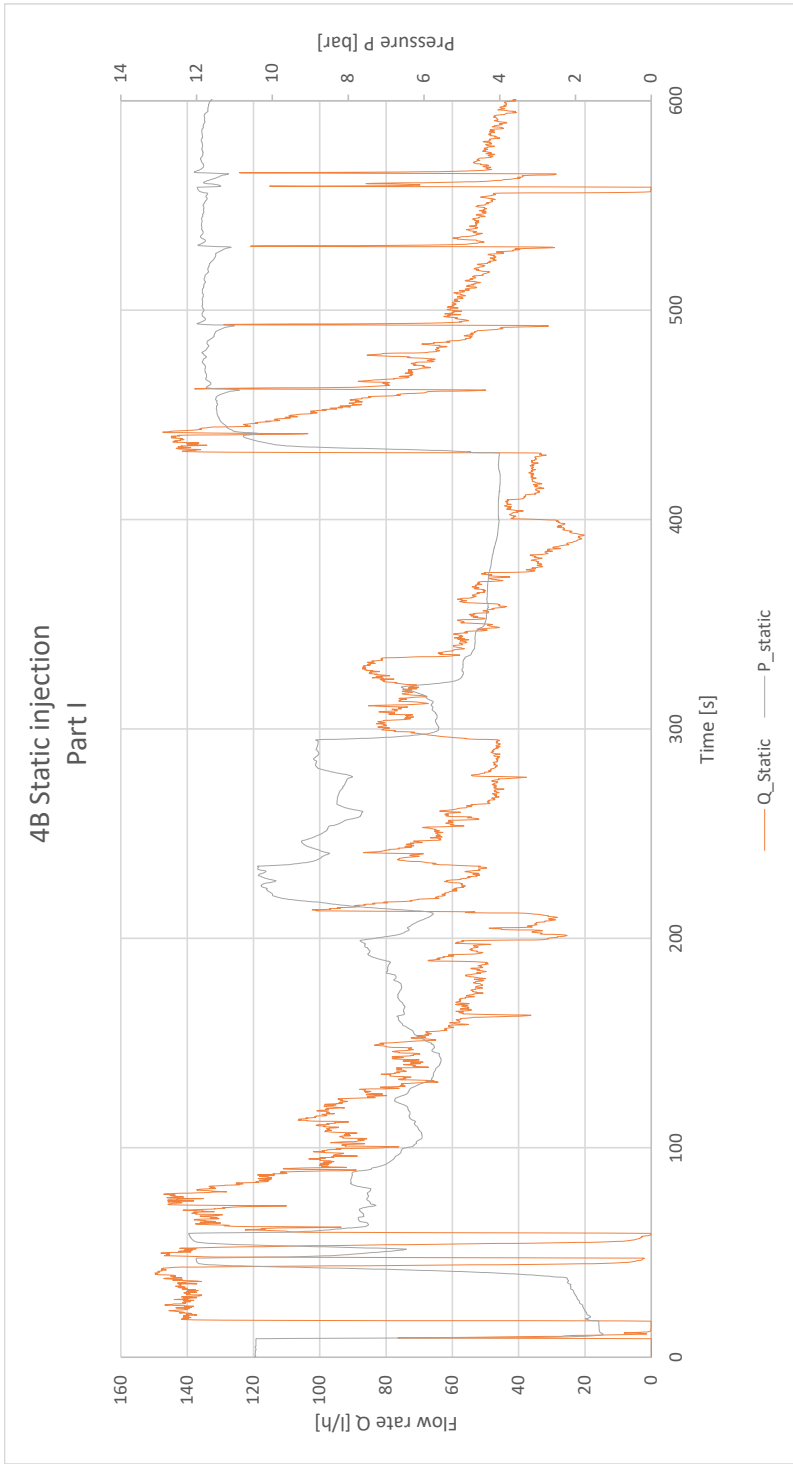
4B Static injection
Part I
Flow rate Q [l/h]
Pressure P [bar]
Time [s]
Q_Static
P_static
0
20
40
60
80
100
120
140
160
0
2
4
6
8
10
12
14
0
100
200
300
400
500
600

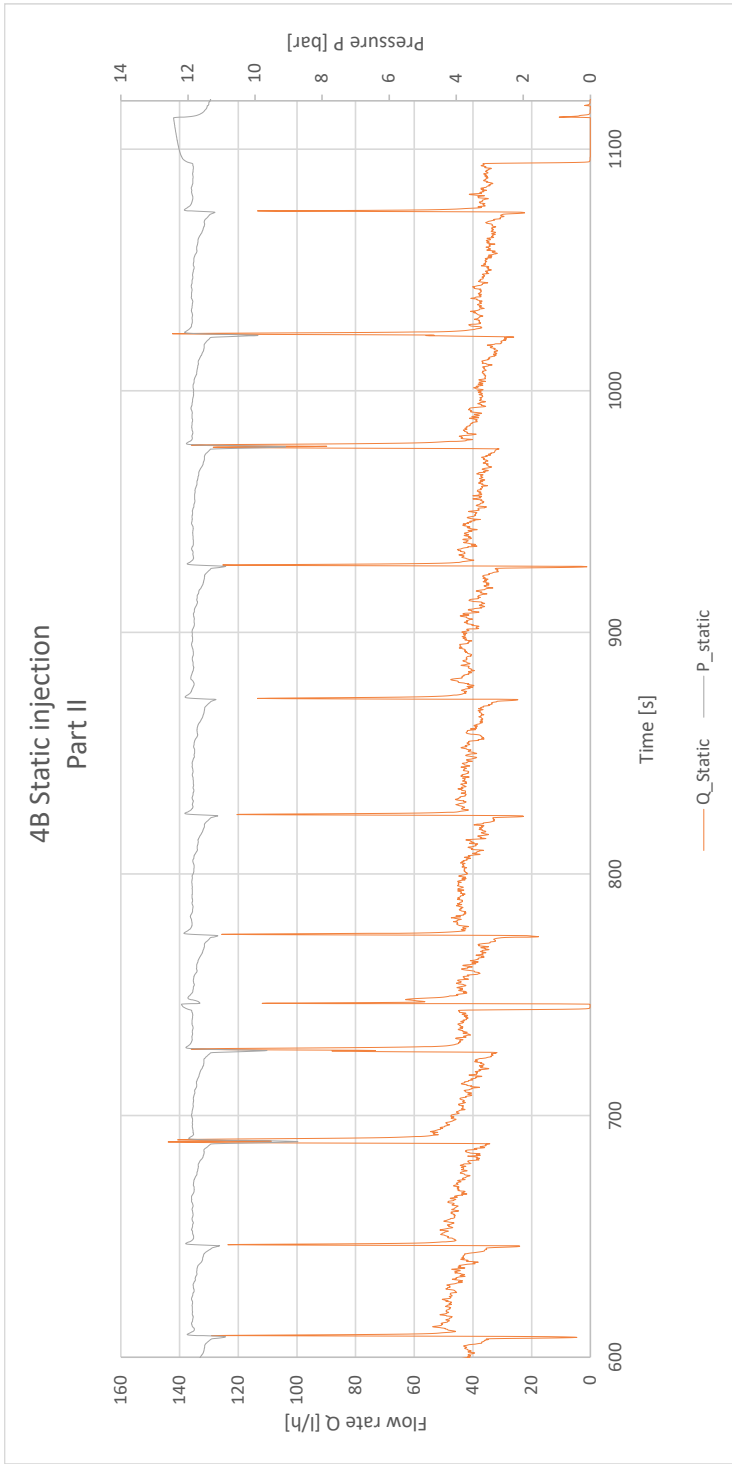
4B Static injection
Part II
Flow rate Q [l/h]
Pressure P [bar]
Time [s]
Q_Static
P_static
0
20
40
60
80
100
120
140
160
0
2
4
6
8
10
12
14
600
700
800
900
1000
1100

BeFo

Box 5501
SE-114 85 Stockholm

info@befoonline.org • www.befoonline.org
Visiting address: Storgatan 19, Stockholm

ISSN 1104-1773